BRNO UNIVERSITY OF TECHNOLOGY
VYSOKÉ UČENÍ TECHNICKÉ V BRNĚ

FACULTY OF MECHANICAL ENGINEERING
FAKULTA STROJNÍHO INŽENÝRSTVÍ

INSTITUTE OF AEROSPACE ENGINEERING
LETECKÝ ÚSTAV

DESIGN OF UNMANNED AERIAL VEHICLE FOR INSECT AEROPLANKTON COLLECTION
NÁVRH BEZPILOTNÍHO LETADLA PRO ODCHYT HMYZÍHO AEROPLANKTONU

MASTER'S THESIS
DIPLOMOVÁ PRÁCE

AUTHOR — **Bc. Vlastimil Hošek**
AUTOR PRÁCE

SUPERVISOR — **Ing. Petr Dvořák**
VEDOUCÍ PRÁCE

BRNO 2017

BRNO UNIVERSITY OF TECHNOLOGY
FACULTY OF MECHANICAL ENGINEERING

Specification Master's Thesis

Department:	Institute of Aerospace Engineering
Student:	**Bc. Vlastimil Hošek**
Study programme:	Mechanical Engineering
Study field:	Aircraft Design
Leader:	**Ing. Petr Dvořák**
Academic year:	2016/17

Pursuant to Act no. 111/1998 concerning universities and the BUT study and examination rules, you have been assigned the following topic by the institute director Master's Thesis:

Design of unmanned aerial vehicle for insect aeroplankton collection

Concise characteristic of the task:

Topic of insect flight, in particular flight related to dispersion and migration mainly by air currents, is highly important and currently studied only by radars. Unfortunately, this type of study does not provide enough information about kind of detected insect. Deployment of unmanned aerial vehicles for catching insect at different altitudes and locations could provide interesting results leading to revelation of time and space distribution of some kinds of insect.

The aim of this thesis is a design of unmanned aerial vehicle for catching of insect aeroplankton. Dimensions of catching device and required characteristics of aircraft will be determined based on the requirements of entomologists from science faculty of Charles university. Catching device will be integrated into the aircraft, with the ability to open and close during flight. Based on this requierements and optimal performance and characteristics in desired flight modes, design of unmanned aerial vehicle will be created.

Goals Master's Thesis:

1. Definition of aircraft and aeroplankton trap requirements.
2. Conceptual design of unmanned aircraft with focus on deployment of insect trap.
3. Aerodynamic design of aircraft considering the insect trap.
4. Evaluation of flight performance characteristics and handling qualities in diverse flight regimes including closed and deployed insect trap.
5. Structural design of the airframe including load assessment.

Recommended bibliography:

ROSKAM J.: Airplane Design: Part I-VIII. DARcorporation, Lawrence, KS, 2006.
CHUN M., NIU Y.: Airframe structural design. Technical Book Company, 1988.

STREETLY M.: (ed.). IHS Jane's All the World's Aircraft. Unmanned 2014-15. Coulsdon, Surrey: IHS Jane's, IHS Global Limited, 2014. ISBN 978-0-7106-3096-4.

DANĚK V.: Mechanika letu. I, Letové výkony. Vydání první. Brno: Akademické nakladatelství CERM, 2009, 293 stran : ilustrace. ISBN 978-80-7204-659-1.

DANĚK V.: Mechanika letu. II, Letové vlastnosti. Vydání první. Brno: Akademické nakladatelství CERM, 2011, 334 stran : ilustrace. ISBN 978-80-7204-761-1.

Deadline for submission Master's Thesis is given by the Schedule of the Academic year 2016/17

In Brno,

L. S.

doc. Ing. Jaroslav Juračka, Ph.D. Director of the Institute	doc. Ing. Jaroslav Katolický, Ph.D. FME dean

Abstrakt
Ke studiu migrace hmyzu a jiných členovců unášených větrnými proudy je výhodné moci sbírat jejich vzorky za letu. Použití bezpilotního letadla s pastí by mohlo být dobrou cestou, jak toho dosáhnout. Tato metoda byla zkoumána a bylo navrženo bezpilotní letadlo v podobě bezocasého dvojploŠníku s pastí umístěnou mezi křídly.

Summary
To study migration of insect and other arthropods in wind currents it is important to be able to collect their samples in flight. Use of unmanned aerial vehicle carrying a trap might be a good method. This possibility was studied and the aircraft was designed as a tailless biplane with trap placed between the wings.

Klíčová slova
Bezpilotní letadlo, Aeroplankton, Odchyt hmyzu

Keywords
Unmanned aerial vehicle, Aeroplankton, Insect collecting

HOŠEK, V.*Návrh bezpilotního letadla pro odchyt hmyzího aeroplanktonu*. Brno: Vysoké učení technické v Brně, Fakulta strojního inženýrství, 2017. 52 s. Vedoucí Ing. Petr Dvořák.

I hereby declare that I eleborated this diploma thesis independently using cited literature.

Bc. Vlastimil Hošek

CONTENTS

1 Introduction **8**

2 History of insect aerial sampling **9**
2.1 Use of airplanes 9
2.2 Other ways of aerial insect collection 10
2.3 Radar monitoring of insect migration 12

3 Requirements **13**
3.1 Flight time 13
3.2 Cruise speed 13
3.3 Stability 13
3.4 Rupture velocity 13
3.5 Transportability 14
3.6 Legal limitations 14
3.7 Take off and landing 15
3.8 Gusts 15
3.9 Maximal banking angle 15
3.10 Summary of requirements 15

4 Preliminary design **16**
4.1 Trap 16
4.2 Single purpose 16
4.3 Propulsion 16
4.4 Wing configuration 16
4.5 Tailless configuration 17
4.6 Manufacturing technology 18
4.7 Aircraft gross weight 19
4.8 Control 19

5 Trap design **20**
5.1 Trap function 20
5.2 Net area 20
5.3 Forces acting on the net 21
5.4 Power required 27

6 Aerodynamic design **30**
6.1 Airfoil selection 30
6.2 Tornado VLM 33
6.3 Stability derivatives 35

7 Structural analysis **36**
7.1 Calculation method 36
7.2 Flight envelope 36
7.3 Wing loading 37

8 Visualization **41**

9 Overall summary and future work recommendations **44**

10 Conclusion **45**

11 List of used symbols **49**

1 INTRODUCTION

The aim of this thesis was the design of an unmanned aerial vehicle for aeroplankton collection. The term aeroplankton encompasses insect and other arthropods, which are carried by the wind. Some of them even intentionally. To be able to collect sample of insects from air is vital for entomologists studying this phenomenon. In past time, they mostly had at their disposal only high ladders, trees and buildings, where traps could be planted. With arrival of affordable UAVs, there is interest to explore the possibility to capture aeroplankton this way.

In cooperation with entomologists of Charles University, namely mostly with Mgr. Jiří Hadrava requirements for such vehicle were formulated. Based on characteristics of various nets and traps and previous attempts of aerial insect collection, the design phase of unmanned aerial vehicle commenced. It was necessary to determine properties of netted insect trap in flight.

Determination of flow through porous screens is currently mostly investigated in association with air filtering. Another field where it is vastly studied is agriculture, where circulation of air in greenhouses is important for optimal growth of plants. Vents or whole walls of greenhouses are often made of porous screens to stop intrusion of insects inside. Significant part of this thesis was focused on this domain, where computation of ideal trap parameters were calculated using MATLAB scripts.

History of insect aerial collection was examined to provide some design inspiration. As this was very unusual task for the aircraft, various aircraft concepts throughout the history were examined. After evaluating requirements and previous experience, the aircraft was designed as a tailless biplane with traps placed between wings.

Aerodynamic analysis and optimization and structural computations were conducted with use of Tornado VLM MATLAB script, with results being further processed by authors own scripts. All MATLAB scripts are attached and can be reused for further optimization. Model design of parts was conducted with use of Catia.

2 HISTORY OF INSECT AERIAL SAMPLING

There are several ways of collecting insect in air. This chapter describes some methods used in the past and their historical evolution. Study of this topic brought some insights on how aerial insect trap can be constructed and what are the most important parameters of its design.

2.1 Use of airplanes

According to P.A. Glick, the first case of an airplane used for insect exploration was at 1926 in Tallulah (USA). During first few flights, researchers collected several insect samples. After these test flights long, 5 year period of insect collecting was conducted. Around 1 000 hours was flown in total of, 1 314 flights, some of them at night.. Researchers recorded flying altitides and how many insects of what specimens were caught. [12]

Airplanes used for the research were DeHaviland H1 army biplanes. traps were installed between the wings. The structure of the wing and the supporting struts had to be stiffened to compensate for increase of aerodynamic forces. This was the reason for the use of for this purpose specially designed airplane Stinson Detroiter SM1 2.1 [12]

Figure 2.1: Stinson Detroiter SM1 monoplane, specially constructed for insect collecting [12]

Several types of traps were developed during the research. They were modified to fit to the wings of various types of airplanes and their efficiency was also improved,

though basic principle stayed unchanged. Trap consisted from five screen-covered frames, where the insects were caught, than two suitable compartments for protecting the screens before and after catching, which was made from aluminum, tin and wood, in later models from steel tubing. [12] On the figure 2.2 one of the trap models can be seen, attached to the plane.

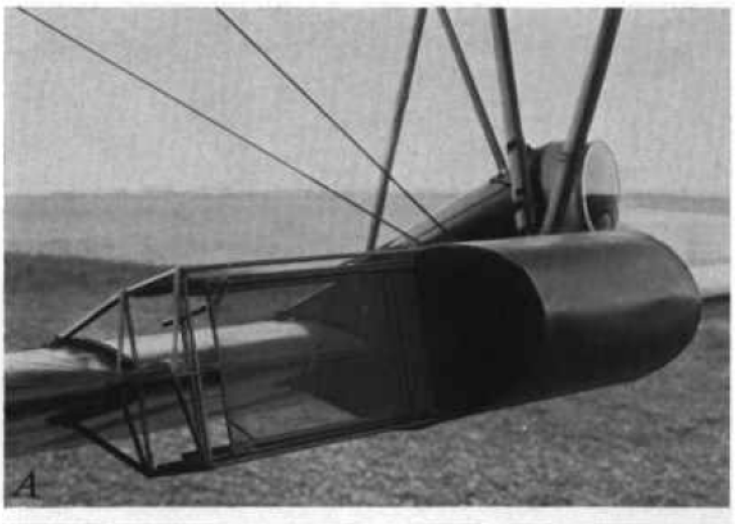

Figure 2.2: A single-compartment insect trap adapted for use on the leading edge of the lower wing of a biplane [12]

Another example of study, where insects was collected with the help of an airplanes and attached traps, was conducted again by Perry A. Glick and colleagues, mainly between 1954 and 1957. During this research 1 552 flights were flown, collecting took about 1 286 hours (flights with nets exposed) and flight altitude was up to 16 000 feet. During the research 35 826 insects were collected. [12]

In this study, slightly modified version of the mentioned trap was used. Later, in 1957 new type of trap was designed. This trap was compounded from series of nets, which were operated from the cabin. An example of this trap attached to an airplane can be seen on figure 2.3.

2.2 Other ways of aerial insect collection

Between 1932 and 1935 a research was conducted which used two kites supporting nets. First kite was a pilot kite: “triangular section box pattern with side wings, having a span of 8 ft. and a height of 8-5 ft.” [14] and was connected by 350 ft. of rope to the second kite, which helped lift the net in mild wind, they could be used separately when wind was strong enough. The nets were attached about 8 ft. below second kite and was designed to be able to open in desired height and closed again before being

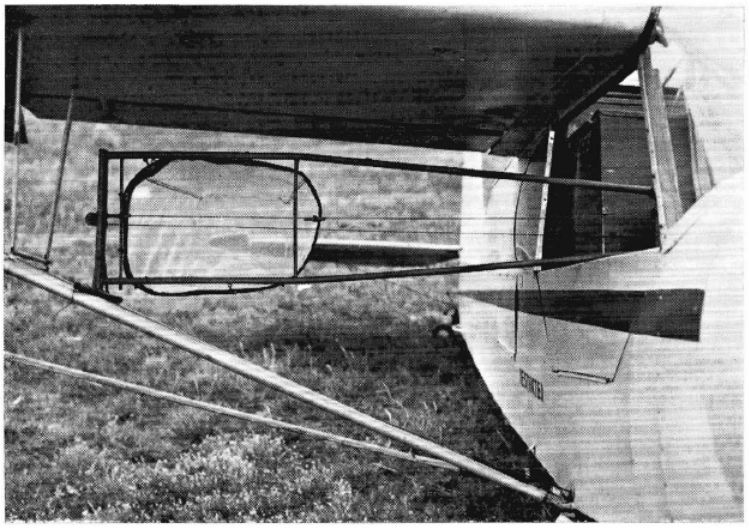

Figure 2.3: Insect trap, steel rails extend from rear of the cabin to the wing strut, where the net is placed in collecting regime. [12]

dropped down, 2.4 The whole mechanism was lifted into the air with help of automobile used as power winch. [14]

Figure 2.4: Closed net being pulled up, attached to the kite [12]

Wireless Station beams in north Lincoln were used for hanging series of nets to collect insects at 1934 and 1935. Wireless station was chosen because it enabled nets

to be deployed in lighter winds than kites could. Samples were collected in different heights by moving the nets on the beams, this enabled the altitude to be kept constant through out the collection. The nets were cone shaped, made of cheese-cloth, 8 ft. long and were held open by a hoop, cords lead to open and closing mechanism. [11]

Net supported by a tethered balloon was used for insect collection during July 1999, 2000 and 2002 at Gread Britain, Bedfordshire. Results of this research were compared with studies of above mentioned Hardy a and Freeman. Collections were done at day and night. As a platform, tethered helium filled blimp at 200 m above ground was used. Tapering net suspended few meters below the ballon was used to collect insect. Net was made from multifilament nylon mesh, same as the collecting bag, which was fastened to the rear end of the net by a heavy-duty zip-fastener. More than 100 hours sampling time was done each year. [17]

2.3 Radar monitoring of insect migration

Another suitable technique for long-term, automatic monitoring of insect migration are radars. It was widely used by entomologists from 1970s. [26] Now the vertical-looking radars (VLR) are used and there is also ongoing research of harmonic radar, which would enable to track individual insect. [18] Monitoring by VLR radar can provide information on size, shape, wing-beat frequency and other. In case of mass migration of one insect species in a large groups it is possible to determine the species. When there is need to collect information about more mixed insects fauna or when the insects are too small to be detected by radar, the direct trapping methods are the only way. [18]

Figure 2.5: Vertical looking radar and harmonic radar [18]

3 REQUIREMENTS

3.1 Flight time

The aircraft should be able to perform sample collection for at least half an hour long continuous level flight. Take off, ascent, descent and landing are performed outside of this time window. Also a small reserve had to be added to the flight time, because of range of operating temperatures of aircraft and battery capacity drop, which is expected to occur after higher number of recharge cycles. Based on these assumptions endurance of at least 40 minutes was chosen as a requirement for the aircraft.

3.2 Cruise speed

To determine optimal cruise speed of the aircraft, various mostly contradictory requirements had to be considered. Optimal cruise speed of the aircraft had to be as high as possible, to enable the trap to filter the highest amount of air. To keep the parasitic drag of the trap at low levels required the speed to be low as well, so the propulsion would be able to provide power for the entire required flight time with batteries of reasonable weight. Another important parameter for successful sample collection which required the cruise speed to be low might have been the rupture velocity of insect.

3.3 Stability

For airplane to be able to fly correctly it has to be stable in the air. This stability could be easily compromised by incorrect placement and dimensions of the trap. Therefore the trap was required to have none or, if desired, small positive effect on stability.

3.4 Rupture velocity

For successful determination of each sample of insect or arthropod caught in the trap, and to find the overall number of samples collected, it was necessary for the insect to stay intact on impact with the trap. This is determined by species of insect in question and the minimal velocity on impact, which its exoskeleton cannot sustain without breaking. This parameter is termed rupture velocity [5] and in aerospace engineering is not unknown.

The rupture velocity is commonly studied in context of adherence of bugs on wings of sailplanes. For high performance modern sailplanes, insect bodies stuck on leading edge of wing can have significant impact on performance. To reduce effect of this phenomenon, leading edges of wings are manufactured with special surface coating, which lowers the adherence of insect. To determine these properties, wind tunnel experiments are conducted, where bodies of dead insect are fired against plates covered

with said materials. For success of these experiments, the insect body is required to rupture on impact and cover the surface with its internal fluids, which then leads to chemical reaction and adhesion of its remains. [21]

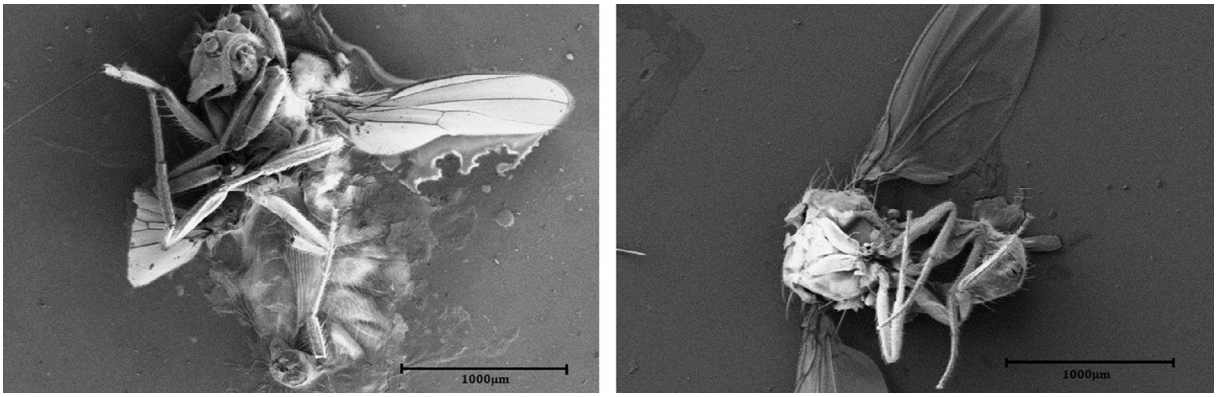

Figure 3.1: D.Melanogaster after impact beyond its rupture velocity [21]

In his study from 1959 W.S. Coleman determined rupture velocity of fruit fly (Drosophila melanogaster), to be 10.7 $\pm$ 0.6 $\mathrm{m\,s^{-1}}$ [5], whereas in study from 2014 by M.Kok. the rupture velocity of D.Melanogaster was found to be at considerably higher value of 24.5 $\pm$ 2.1 $\mathrm{m\,s^{-1}}$. [21] Examples of impact beyond this velocity are depicted on 3.1. As explained further in chapter 5.1, this velocity threshold ultimately didn't pose any limits in regard to the aircraft design.

3.5 Transportability

To be able to provide insect collection at various locations, the aircraft needs to be transportable. This could be accomplished by either small size of the aircraft, or by its dismountability. Sample collections are to be conducted at one location at a time for consecutive longer time intervals. Therefore there is small need for rapid deployment after transportation. For this reason, the aircraft was allowed to be dismantable, in case it leads to increase of performance over small unbreakable aircraft. Maximal length of one segment was set to 1000 mm, as at this size, it will be still easily transportable by ordinary car.

3.6 Legal limitations

According to amendment X of regulation L2, issued by CIVIL AVIATION AUTHORITY Czech Republic there are some altitude limitations for remotely controlled RC aircraft and UAVs on the territory of Czech Republic. Maximal operating altitude of remotely controlled aircraft is 300 m AGL. There are also limitation regarding distance from men and obstacles, which are not applied for aircraft of maximal take off weight

under 7 kg. These limitations would made impossible some desired sampling regimes, which led to restriction of the maximum take off weight of the aircraft to 7 kg. [7]

3.7 Take off and landing

Decision to further limit aircraft weight was based on the take off and landing procedure This is to be conducted several times a day. Preferable take off is from operators hand, if this cannot be achieved, alternatively rubber band catapult can be used. Belly landing will be used to recover the aircraft. Therefore the aircraft weight was further limited to 5.5 kg

3.8 Gusts

The cruise speed of the aircraft is expected to be very slow, therefore strong gusts will have great effect on flight performance and loading factor. Gusts of 10 m/s were considered at the V_C, 6 m/s at V_D.

3.9 Maximal banking angle

The aircraft is not expected to undertake any aerobatic maneuvers and all sample collection is expected to be done at level flight at cruise speed, therefore the maximal banking angle was set to 60°, which is in accordance with what is allowed to piloted general aviation airplanes.

3.10 Summary of requirements

Parameter	Value	Unit
max. Weight	5.5	kg
min. Endurance	40	min
max. Segment length	1000	mm
max. Cruise speed	20	m/s
Operating altitude	0 to 300	m AGL
Gust speed	10	m/s
Trap control	remotely by operator	

Table 3.1: Table of requirements

4 PRELIMINARY DESIGN

4.1 Trap

Many trap variants were considered, based on present ways of insect collection and designs used in earlier attempts mentioned in chapter 2. The need to operate opening mechanism during flight had the biggest impact on the final design of the trap. It required to incorporate movable parts into design, very large such parts, in case of opening and closing of the whole trap. This would considerably lower structural rigidity of the trap. Therefore it was decided to open and close only small segments of the trap. Because of the need of preserved stability of the aircraft the sweptback net between the wings, in more detail described in chapter 5.1, was selected as a best option.

4.2 Single purpose

One of the advantages of unmanned aerial vehicles over piloted aircrafts is their relatively smaller size, which correlates with lower manufacturing costs. This fact opens the economic possibility to create many single purpose UAVs, rather then one larger multipurpose vehicle, as is the case of earlier mentioned piloted aircrafts.

Classical UAVs are mostly designed as a single purpose vehicles Classical aircraft, be it a tailed aircraft, flying wing or any other existing UAV, this required new unmanned aerial vehicle to be build around the device, similarily as in the case of Fairchild-Republic A-10 Thunderbolt II, where the airplane was constructed around a required device - GAU-8 rotary cannon. [19]

4.3 Propulsion

As stated in 3.4, it is vital, that the insect stays intact after capture. This requires correct placement of the propeller, so the insect heading to the net does not come in contact with it. It could be achieved by use of two or more puller motors on wing far from the trap, or to place the motor behind. Because of understandable desire to use only one motor, aft pusher propeller configuration was selected as the best form of propulsion.

4.4 Wing configuration

To secure rigid construction of the trap, it was necessary to have either very rigid frame connected on the wing or to place the trap between the wings of a biplane. Because of decision to make most of the net static, as discussed in 4.1 the biplane configuration with net between the wings was selected as a best solution.

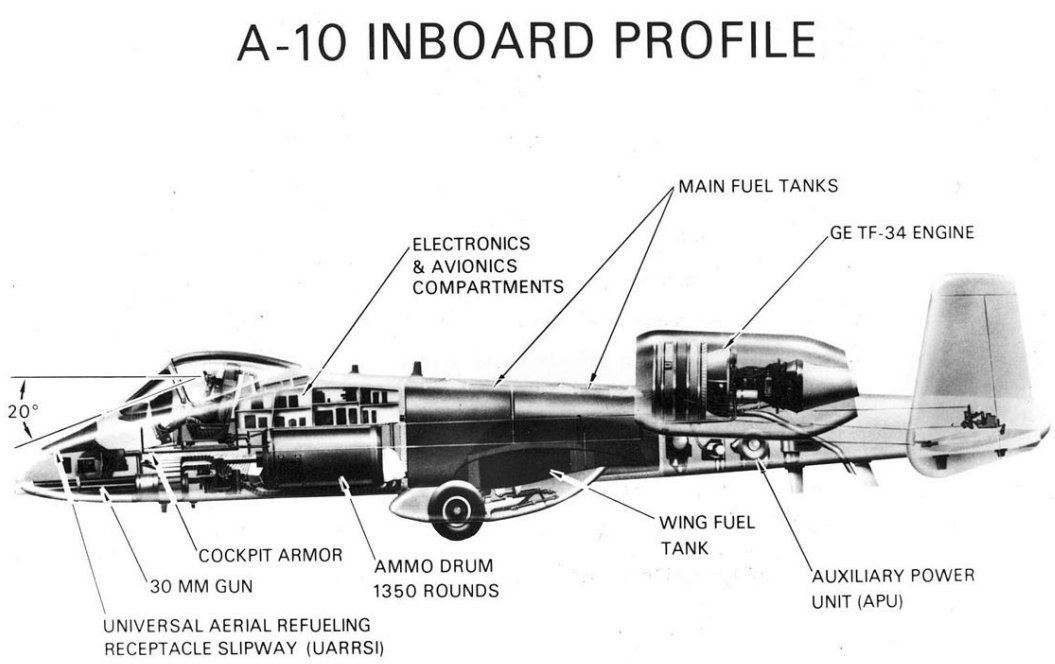

Figure 4.1: A-10 Thunderbolt II [1]

Advantage of a biplane over a monoplane is its potential structural rigidity and better climb rate, of course, compensated by higher drag. As the cruise speed is in this case very low and most of the drag is created by the trap, biplane design advantages can be exploited with little cost.

For vertical gap between biplane wings of 1 chord length and larger, the mutual interference effect of wings is small and wings act as individual lifting surfaces. [20] So it was vital to get as close to gap of one c. This demand was met only partially, as is clear from chapter 7. where at the root of wing the gap is slightly smaller than the root chord length.

4.5 Tailless configuration

For the trap to have enough frontal area, it was vital to use wing or wings as a support structure. As the trap in this position it was vital, for the trap to provide lateral and directional stability. This was achieved by placing the trap slightly behind the CG diminishing the need for horizontal stabilizer on the tail. Therefore it was decided to use flying wing configuration. In search for use of such configuration in history, several similar airplanes were found, from which Dunne D.8 was the most iconic example.

Existence and success of Dunne D.8 and its successors brought confirmation that it is possible to build and successfully fly a tailless biplane.

Figure 4.2: Brugess Dunne BD-1B - designed by John William Dunne [28]

4.6 Manufacturing technology

Wings and fuselage are made of hot-wire cut PPS foam core, positively laminated with fiberglass. Wings and trap are supported by carbon fiber and wires of nylon braided line. Wing connection points, motor mount, trap mechanism and other parts are 3D printed, made of ABS plastic. The wing end plates are made of light plywood.

4.7 Aircraft gross weight

The estimation of aircraft parts mass was made based on UAVs previously built at Institute of Aerospace engineering and earlier experience of author. List of masses of individual components can be seen in table 4.1.

Component	**Mass** g
Airframe including Trap	1800
Motor	300
Propeller with adapter	55
Receiver battery	110
Elevon servos	120
Trap servos	80
ESC	80
Wiring	80
Receiver, sensors	50
Flight control, telemetry, GPS, Power module	150
Total mass without propulsion battery	2825

Table 4.1: Estimated mass of individual segments

The most influential portion of aircraft gross weight was the weight of the battery used for propulsion. This value was not so easy to estimate and is dealt with in more detail in chapter 5.1.

4.8 Control

The aircraft will be remotely controlled by classic RC transmitter and receiver. During flight it is possible to hand over the control to automatic flight control unit. As a flight control system, Pixhawk PX4 (displayed on figure 4.3) was chosen because of familiarity of with Ardupilot FC family, of which Pixhawk is descendant of.

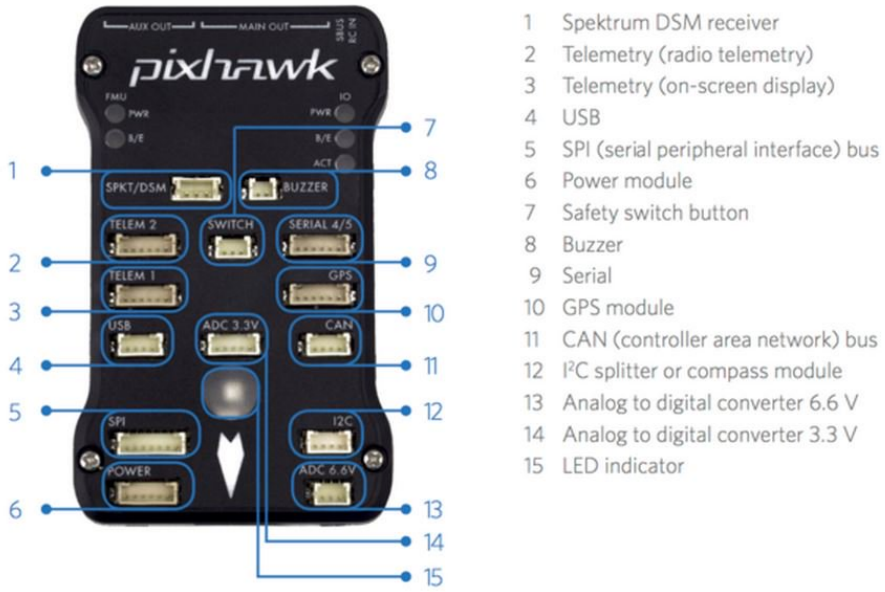

Figure 4.3: Pixhawk flight control [27]

5 TRAP DESIGN

5.1 Trap function

Important factor was the need to be able to open and close the trap during flight. Flight time with closed trap is negligible compared to the actual collection time with open trap. This led to use of static, permanently fixed main part of the net. This main part is attached between the top and the bottom wing and for ease of transportation, split in the middle, where wings are connected to the fuselage. It is swept at an angle (greater than the wings), so the insect hit by the net slides to its outer edge, where it is collected. The sample collection ability is provided by two bug bags, each placed at the outer end portions of the net. The opening and closing is operated by servos. The bug bags, ideally full of samples, are detached after landing and replaced with unused ones.The trap can be described as a flying insect snowplow with ability to collect the plowed insect.

5.2 Net area

In contrary to what most airplane designers are trying to achieve - to minimize the frontal area of an airplane, for purpose of airplane collecting aeroplankton it is vital the frontal area of the trap will be as large as possible. This will enable the aircraft to sweep large volume of air through the net, increasing overall number of samples collected.

This goal of course carries a problem of higher drag, which has to be compensated for by more powerful propulsion unit.

Net material

Aerial (also often called Butterfly) nets used by entomologists to collect insect are often made of soft polymer mesh. Light net bag is attached to a round light steel frame connected to a rod, which is held by hand. Capture is done by swinging the net at insect flying nearby. [25]

For butterflies and larger insect, lower density of threads is required, so the net can be made lighter, which diminishes the possibility of damaging the specimen. On the other hand, to enable the opportunity to capture even very small arthropods the meshes of some nets may require to be made very fine. From aerodynamic point of view, even with the lever effect of the rod, the swing of the net is still done at quite a low speed, so no aerodynamic optimization of the mesh is usually needed for standard nets.

This however may not be the case of insect collection from aerial vehicles. In the aerial sampling by J.W. Chapman mentioned earlier, nets and collecting bags suspended from blimps were made of multifilament nylon mesh [17]. Multifilament mesh can have good structural and deep filtration properties and are easier to manufacture, but their aerodynamic qualities are worse, compared to monofilament meshes of the same material. For this reason nylon monofilament thread was chosen as the material of the net.

Catalogs of several manufacturers were examined and based on technical parameters of the products, mesh materials of SEFAR company were found to best suit aerodynamic requirements. The choice of materials was based on open area percentage and on mesh opening, where values around $300\,\mu\mathrm{m}$ and lower were considered. Their parameters can be found in 5.1.

From many mesh materials listed in the catalog of manufacturer Sefar, 8 materials were selected for calculation. The selection was based mainly on the most important factor - the mesh opening value α, which is determined by the ratio of the open areas to whole area of the mesh [29]:

Another important factor for material selection was the micron value of the mesh. This parameter determines the size of the smallest solid object, which can pass through the material.

5.3 Forces acting on the net

To estimate this drag force, analysis of various mesh materials at different velocities and angles of the net was calculated, using MATLAB software. For this analysis the method proposed by [4] was used, with some changes based up was based upon the For this preliminary analysis, curvature of the net due to airfoil camber was neglected and top and bottom edge was considered a straight line.

Mesh	**Opening**	**Open area**	**Mesh count**	**Yarn ϕ**	**Weight**	**Thickness**
	μm	$\%$	n/cm	μm	g/m^2	μm
17-600/70	600	73	14	100	101	180
07-240/59	240	59	32	73	35	115
06-600/59	600	59	13	180	80	350
17-115/58	100	58	73	38	17	50
03-190/57	190	57	40	62	30	100
06-475/56	475	56	16	180	85	290
07-285/55	285	55	26	103	60	168
07-105/52	105	52	69	42	25	63

Table 5.1: Table of mesh materials

Viscosity of air μ is highly dependent on temperature and can by obtained from Sutherland's formula (5.1), where T is input temperature, C is Sutherland's constant for the air and λ is constant for the gas, calculated from reference viscosity μ_0 at reference temperature T_0 by equation (5.2) and for air is equal to $1.512\,041\,288\,\mu\text{Pas/K}\sqrt{(2)}$ [31]

$$\mu = \lambda \frac{T^{\frac{3}{2}}}{T + C} \tag{5.1}$$

$$\lambda = \frac{\mu_0 \left(T_0 + C\right)}{T_0^{\frac{3}{2}}} \tag{5.2}$$

$$\Delta p = \frac{1}{2} \rho k_p v^2 \tag{5.3}$$

this references equation (5.3).

Pressure loss coefficient can be obtained from equation (5.4) proposed by E. Brundrett [4] for metallic mesh and later modified by Bailey [3] for calculation of insect-proof screens.

$$k_p = \left(\frac{1 - \alpha^2}{\alpha^2}\right) \cdot \left[\frac{18}{Re} + \frac{0.75}{log\left(Re + 1.25\right)} + 0.055 log\left(Re\right)\right] \tag{5.4}$$

Reynolds number expresses the ratio of inertial and viscous forces [9] and for our purposes can be calculated by equation (5.5), where v is the free stream velocity, ν represents the kinematic viscosity of air, and the length factor is defined as yarn thread diameter of the mesh d. [32]

$$Re = \frac{vd}{\nu} \tag{5.5}$$

To incorporate the effect of angle of the net, it was necessary to correct the loss coefficient using equation (5.6) proposed by Laws and Livesey, where ϕ is the angle of attack of the net, for which the equation is applicable up to the value of 42° [22].

$$k_{p\phi} = k_p cos^2 \phi \tag{5.6}$$

Use of net at various angles was considered. Angle was necessary to enable the insect to slip in to the bug bag. Illustrative image generated during calculation can be seen on figure 5.1

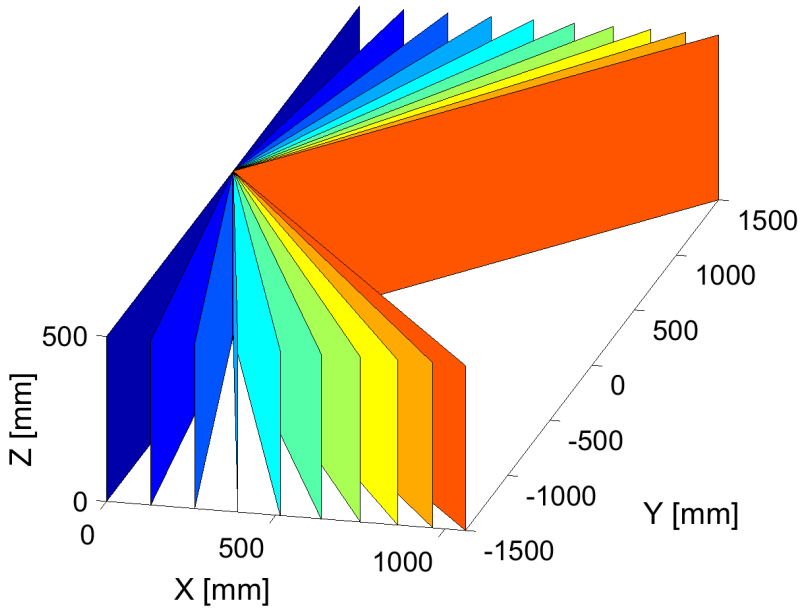

Figure 5.1: Net at different angles

Meshes have different thread diameters, therefore for each mesh and each velocity Reynolds number had to be calculated 5.2. Thie above mentioned equation 5.4 was used to calculate pressure loss coefficient of each mesh 5.3

Using Bernuli equation pressure drop over the mesh could be calculated (figure 5.4). This was important for determination what mesh would the best. After consideration, the mesh 07-240/59 was selected for use. The characteristics of selected mesh are presented in figure 5.5.

After selection of the best mesh material another faze of iterative computation would begin. Its result was estimation of Drag caused by the mesh at different frontal areas and velocities.

$$C_D = C_{D0} + C_{Di} \tag{5.7}$$

where C_{D0} is zero lift drag coefficient and C_{Di} is induced drag.

In this case, parasitic drag of the net is very large in comparison with parasitic drag of the aircraft or induced drag. As is lated shown by figure 5.8

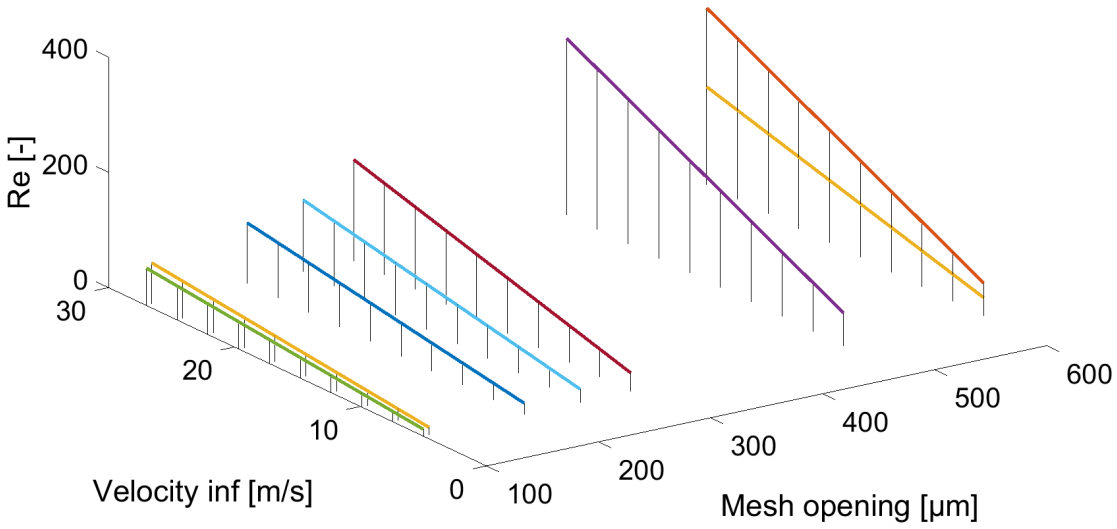

Figure 5.2: Reynolds number of meshes

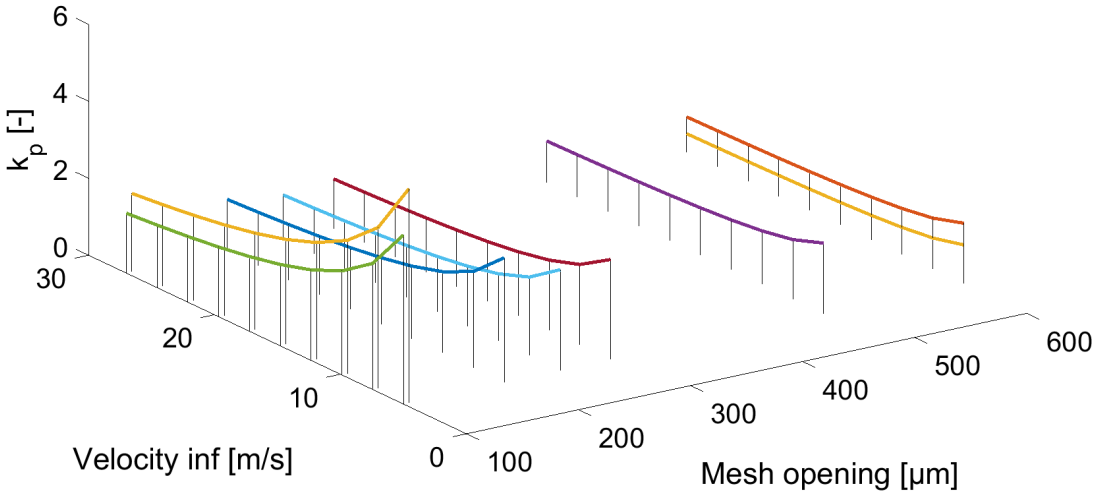

Figure 5.3: Pressure loss coefficient of meshes

As was stated by in at aerodynamic for engineers lower speeds induced drag dominates, therefore the parasitic drag could be neglected and only induced drag and drag caused by the trap were considered for further calculations.

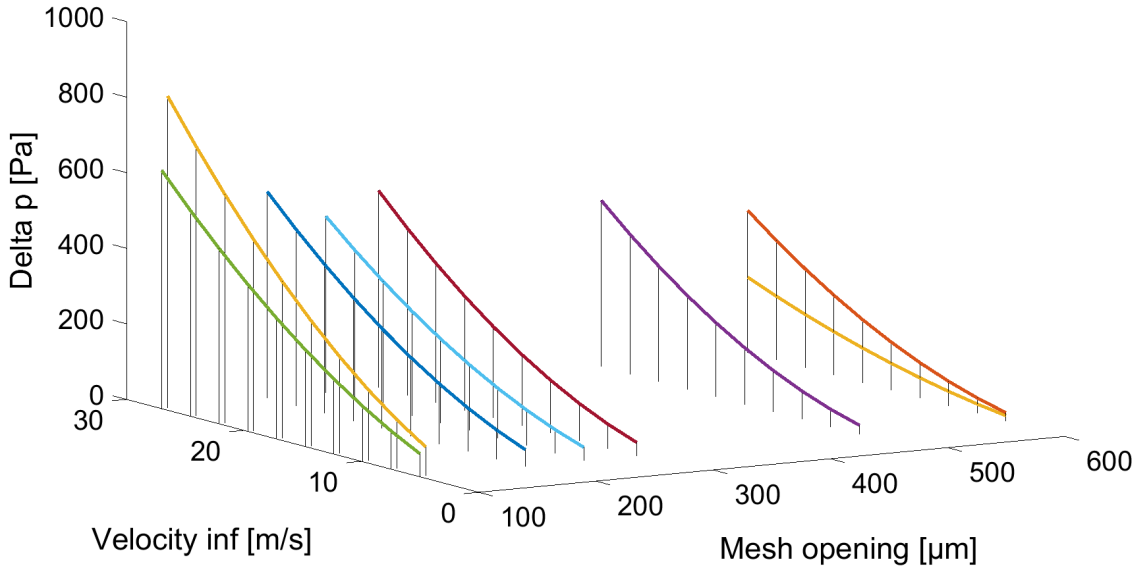

Figure 5.4: Pressure difference of meshes

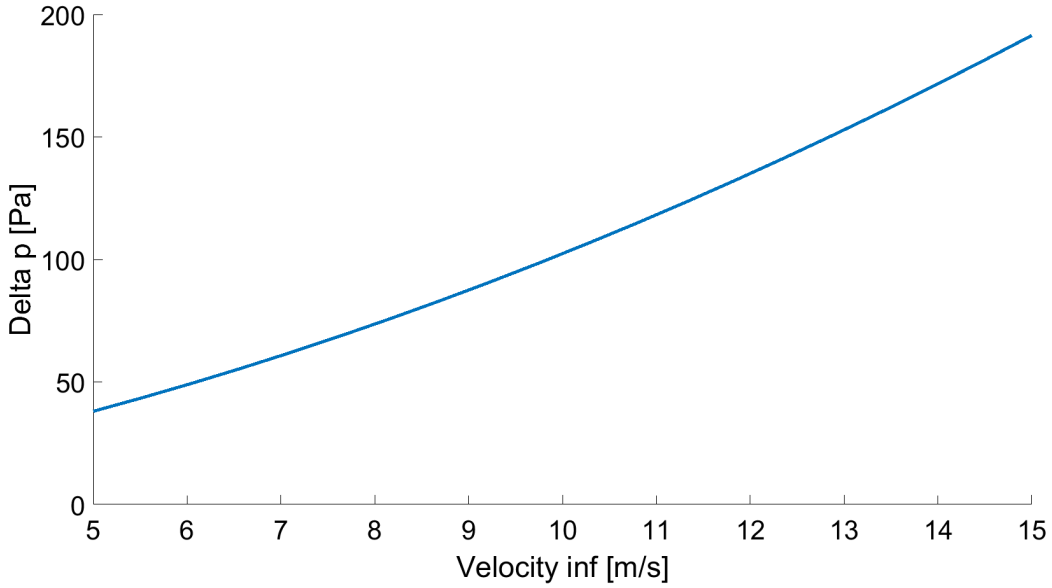

Figure 5.5: Pressure difference of selected mesh

Because of the slow cruise speed, it was assumed that the parasitic drag of the airplane will be considerably smaller than the parasitic drag caused by the trap, therefore for preliminary calculation of aerodynamic characteristics, this drag was neglected.

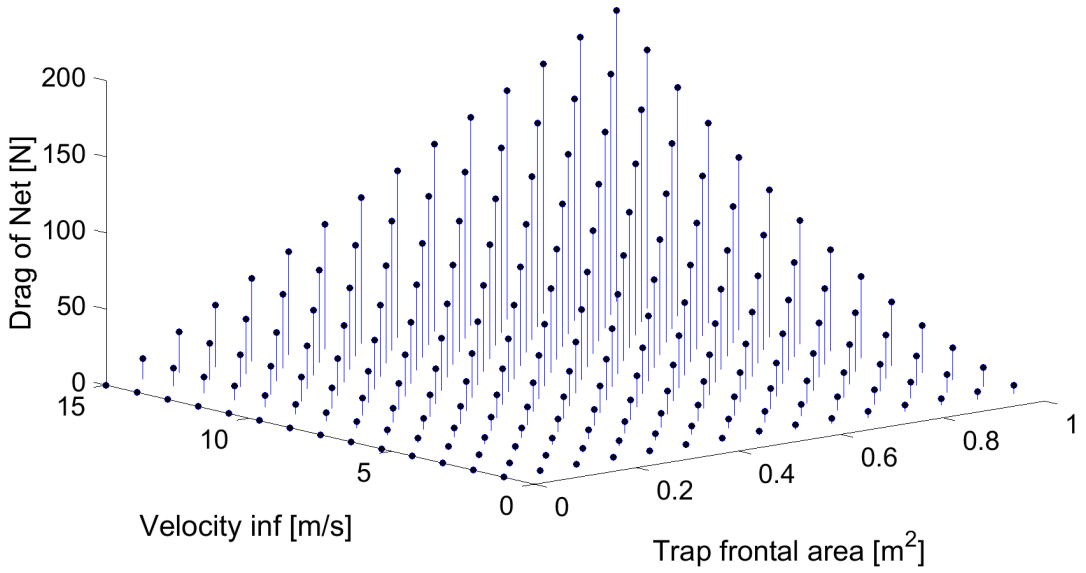

Figure 5.6: Drag as a function of net frontal area

This allowed the possibility to use Vortex lattice method, which is useful for determination of induced drag from lift, but cannot deal with parasitic drag of an airplane.

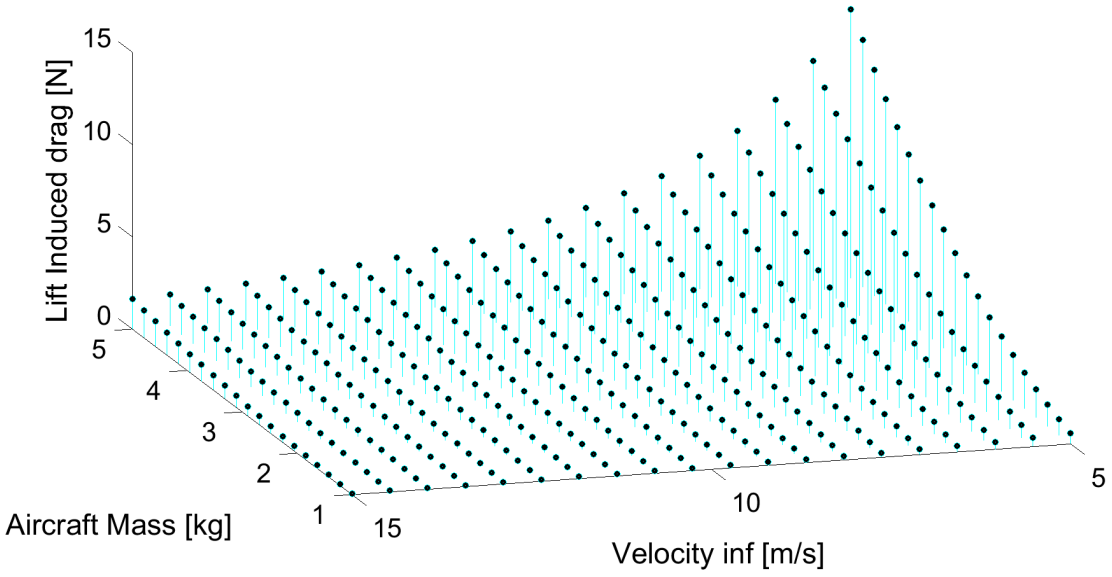

Figure 5.7: Lift induced drag

5.4 Power required

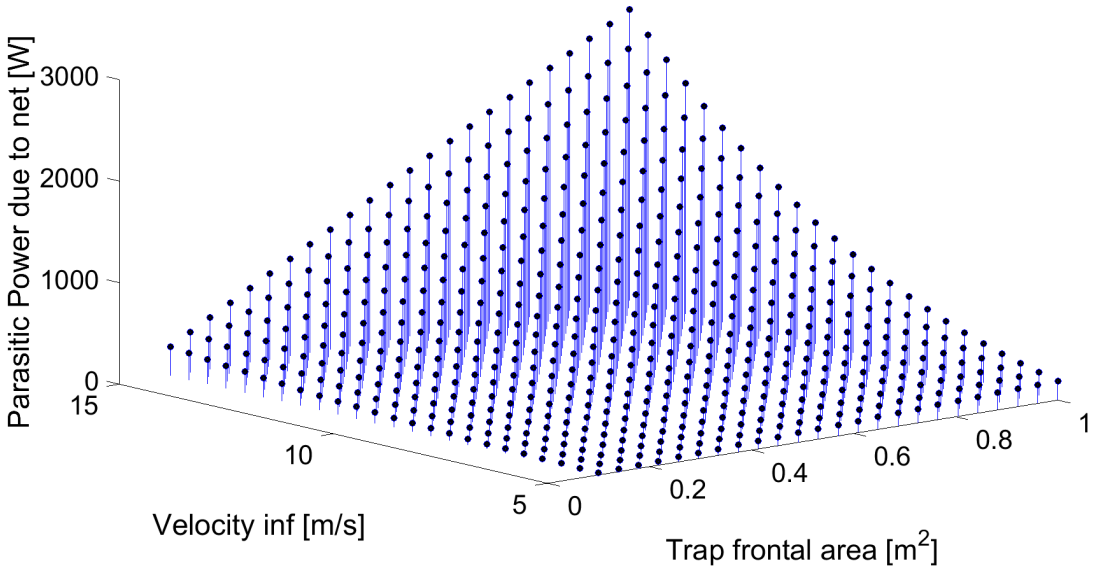

Figure 5.8: Parasitic power

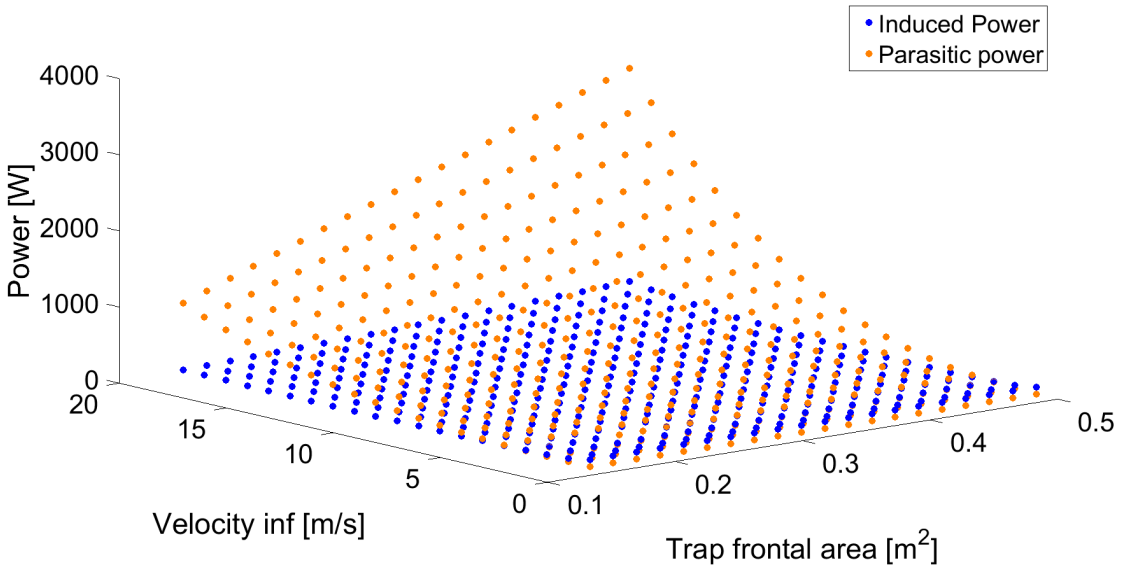

Figure 5.9: Comparison of induced power and parasitic power caused by the net

Based on the required power and flight time, and with consideration of Li-pol battery average power ratio of 150 [Wh/kg], battery weight was calculated.

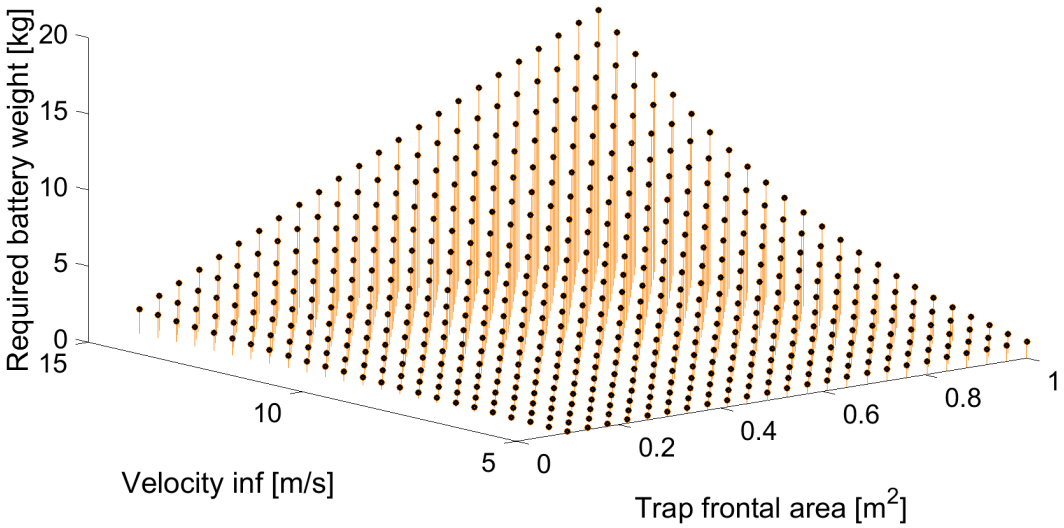

Figure 5.10: Battery weight required by the parasitic power of the net

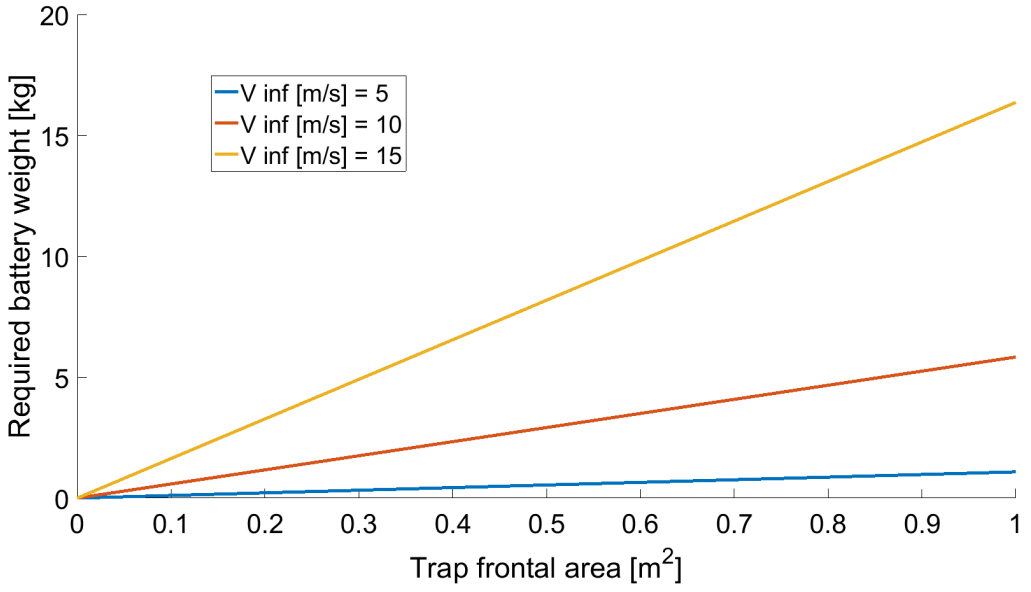

Figure 5.11: Battery weight required by parasitic power for selected free stream velocities

After consideration of all calculated values and another iterative process of fine tuning, cruise speed V_C of 12 m/s was chosen. This led to use of battery of weight around 2.5 kg to 40 minute flight.

6 AERODYNAMIC DESIGN

6.1 Airfoil selection

The absence of the empenage of flying wings leads to benefits of lowering the parasitic drag and overall structural weight of the aircraft, however it also carries some disadvantages. The most significant is the higher difficulty for flying wing to preserve stability. There is no downward acting force on the lever, so different instrument to preserve stability needst to be incorporated. One of the most used is the lowering of airfoil pitching moment coefficient Cm to values close to zero. This can be achieved by selection of reflexed airfoil. This advantage is, as allways in aviation, ballanced by some handicap. In this case it is the lower airfoil lift coefficient Cl, than non-reflexed airfoil possesses.

Based calculation of cruise speed by the use of methods from [8] it was necessary to chose airfoil which can operate well enough in low Reynold's number region.One of the advantages of selected biplane design was the lower wing loading, in comparison to monoplane. Another important benefit stemmed from inherent structural stiffness the biplane design provides which led to possibility of selection of thinner profiles, than is common for flying wings.

This led to survey of thin, low Reynold's number reflexed airfoils. Thin reflexed airfoils are often used for light gliders at various competitions. Disadvantage of most of these airfoils is the lack of wind tunnel data. Most of the data avillable are calculations with usage of programmes Xfoil by Professor Mark Drella of MIT or PROFIL by Professor Richard Eppler uf University of Stuttgard. [15]

Several reflexed airfoils were examined, and mostly airfoils created by Dr. Martin Hepperle and Hartmut Siegmann were chosen for more detailed inspection. List of their characteristics can be found in table 6.1.

Airfoil	**Camber**	**Thickness**	cm_0	a_0
Re 200,000	%	%		°
MH44	1.5	9.66	+0.0050	-0.34
MH45	1.65	9.85	+0.0070	-0.27
MH60	1.76	10.08	+0.0030	-0.31
TL55	1.90	9.44	-0.0052	-0.68
S5010	2.20	9.83	+0.0080	-0.52
HS 522	2.01	8.67	-0,0050	-0.84

Table 6.1: Narrow selection of considered airfoils [30]

After study of calculated characteristics and description of these airfoils [30], some of them were calculated and compared using Airfoiltools website [2]. Three airfoils were compared at Reynolds numbers of 50,000, 100,000, and 200,000. This comparison at Re 50,000 can be seen in figure 6.2. As a result of this comparison, the airfoil MH44 was selected for use on the aircraft, because of its good behavior in the low Reynold's

number region. This airfoil was used on both root and the tip and wing twist is achieved only geometrically by the rotation of the tip profile by angle of -3°. Its outline can be seen in figure 6.1.

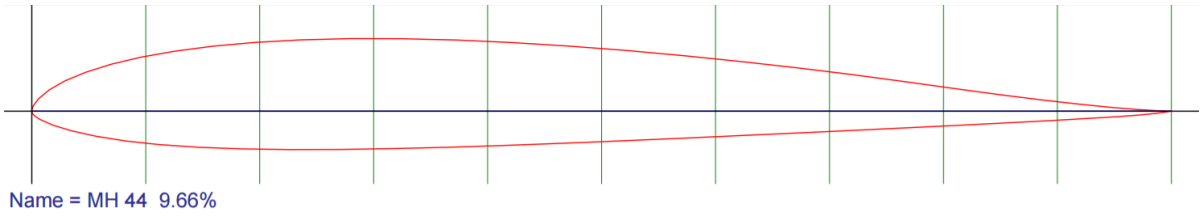

Figure 6.1: Airfoil MH 44 [2]

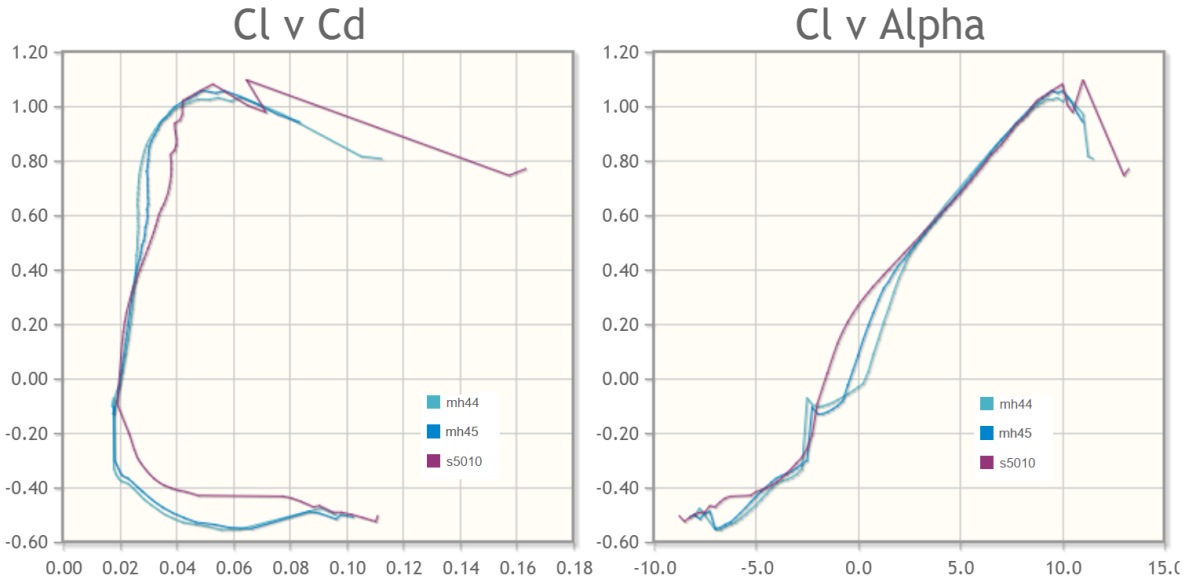

Figure 6.2: Comparison of selected airfoils at low Re [2]

After with selected airfoil, long iterative process of was required for optimal setting of various variables. During this process it was necessary to know characteristics of selected airfoil at various speeds, therefore detailed analysis of airfoil MH44 was performed by use of XFLR5 airfoil analysis tool. Results are plotted in figure 6.5.

MATLAB and Tornado VLM code were also used to tune the final dimensions of the aircraft. After number of iterations final dimensions were fixed, these can be seen in table 9.1. Position of CG was placed to 20% of mean aerodynamic chord as this is expected to produce good results. [24]

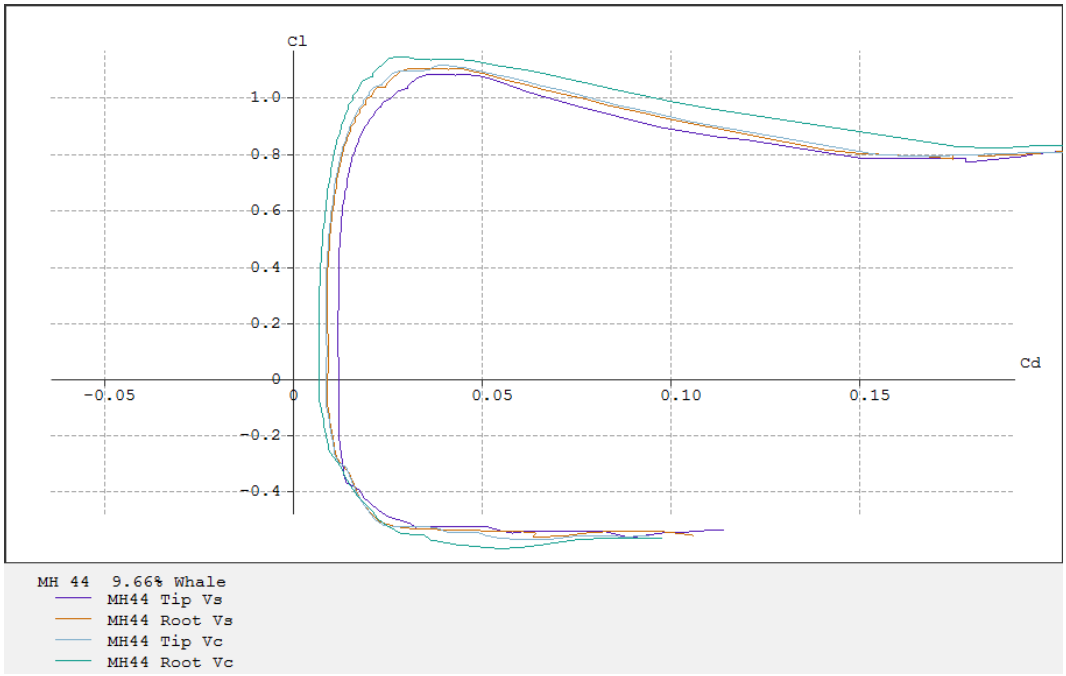

Figure 6.3: MH 44 polar at relevant Re

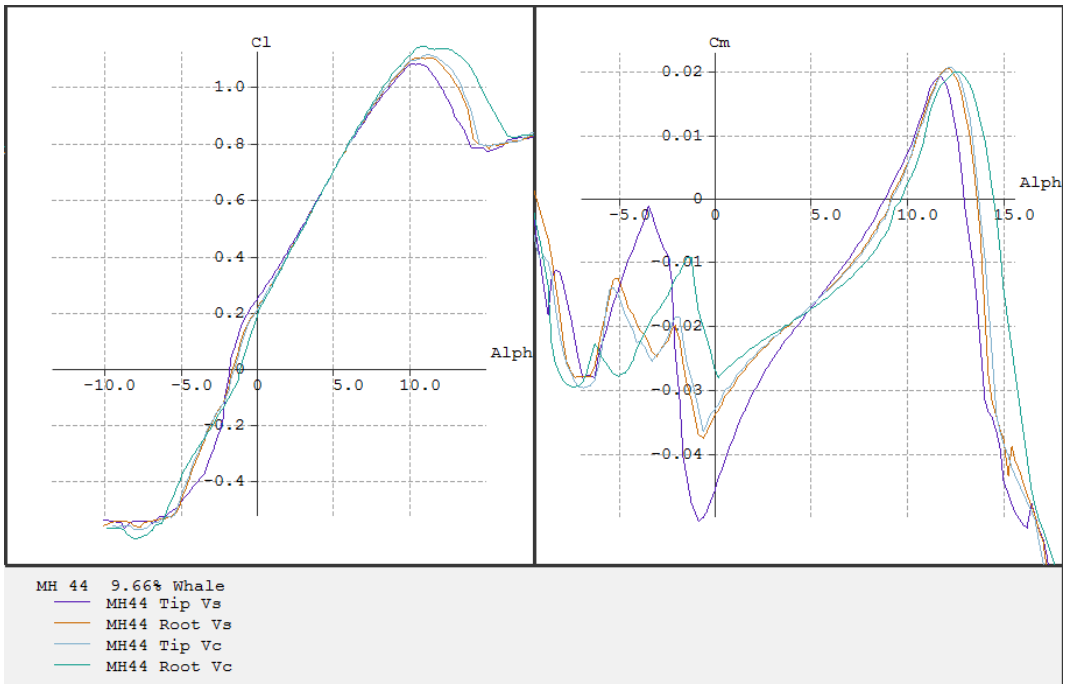

Figure 6.4: Comparison of Cl and Cm by angle of attack at relevant Re

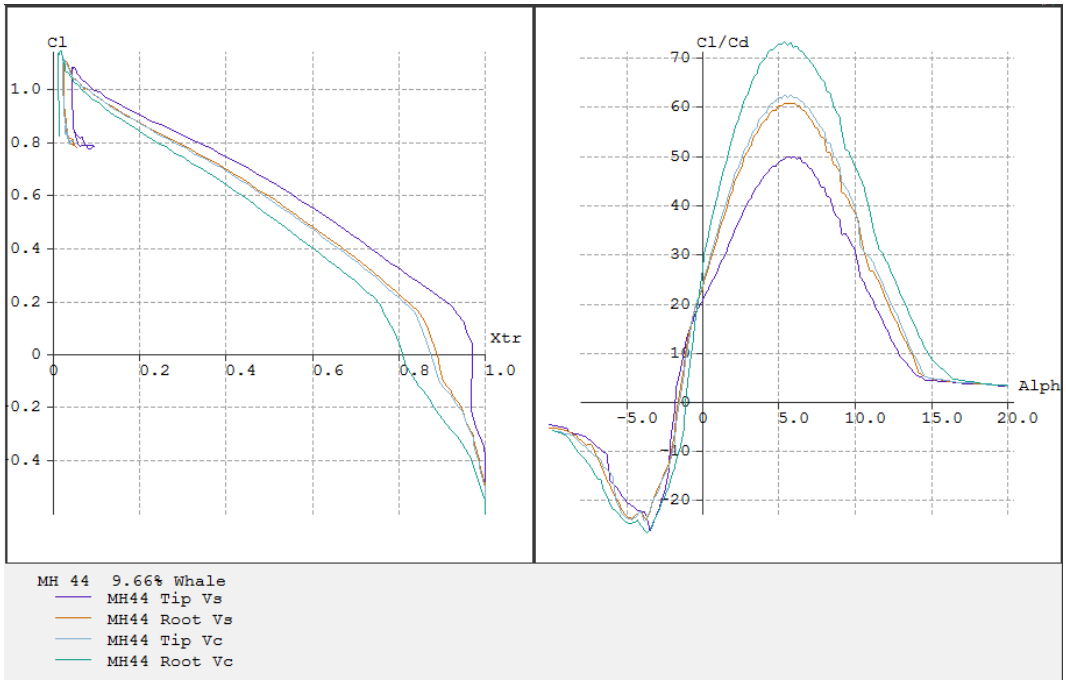

Figure 6.5: Location of transition point and dependance of Cl/Cd on angle of attack

Dimension	Value	Unit
Airfoil	MH 44	
Wingspan	2.2	m
Wing Area (one wing)	0.715	m^2
Root chord	0.4	m
Tip chord	0.25	m
Aspect Ratio		-
Tapering	0.659	-
Leading edge sweep	24	°
Wing twist	-3	°
MAC length	0.33	m
Center of gravity x position	0.27	m
Aircraft gross weight	5.275	kg

Table 6.2: Aircraft geometric parameters

6.2 Tornado VLM

Because of the sweep of the wing and biplane configuration, classical lifting line theory could not be used with significant accuracy. Vortex lattice method was selected as a toll to provide results with enough expected accuracy. As quite good, although hard to handle, was found to be Tornado VLM MATLAB code by Thomas Melin [33].

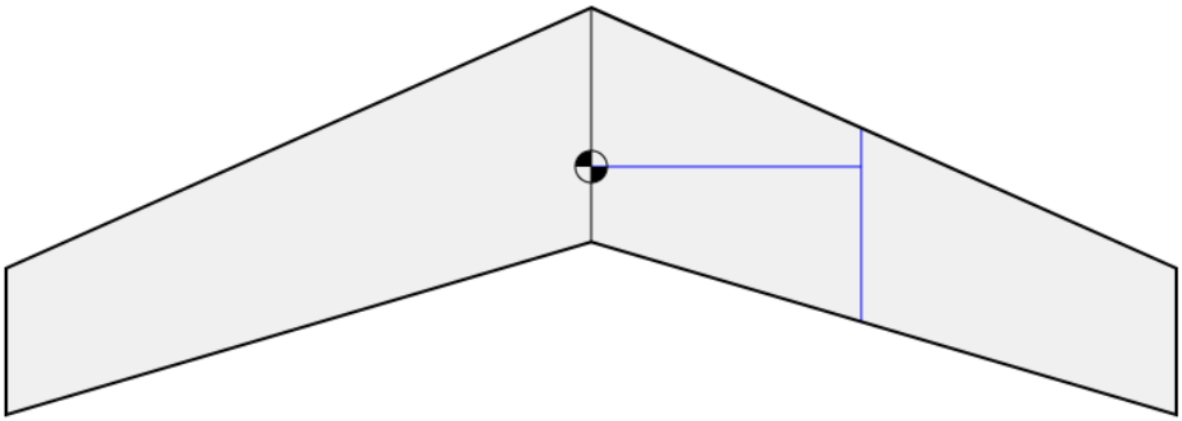

Figure 6.6: Top view of the wing created using [10]

Advantage of this code is that results are imported straight to MATLAB Workbench and calculations can be applied directly and programmatically. Tornado VLM was used together with authors own code to optimize the design and calculate aerodynamic forces.

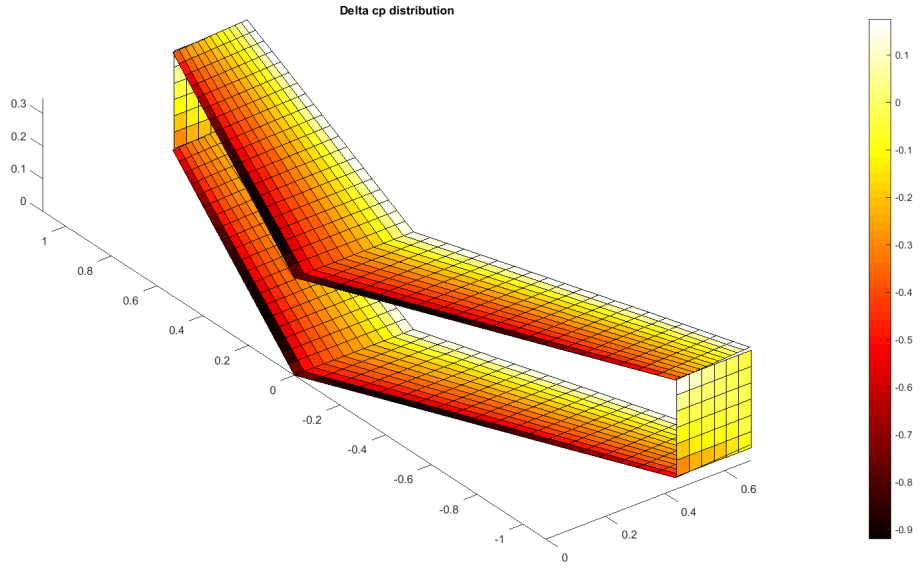

Figure 6.7: Pressure difference on the wing created using Tornado VLM script

6.3 Stability derivatives

Tornado VLM can estimate stability derivatives, these were estimated only for use without the trap. Derivatives for flight with the net will need to be measured in flight.

TORNADO CALCULATION RESULTS, Derivatives

Reference area:	0.715	α [deg]:	5	P [rad/s]:	0
Reference chord:	0.33077	β [deg]:	0	Q[rad/s]:	0
Reference span:	2.2	Airspeed:	12	R[rad/s]:	0

CL derivatives :		CD derivatives :		CY derivatives :	
CL_{α}	7.1405	CD_{α}	0.25727	CY_{α}	-1.2447e-13
CL_{β}	4.5711e-06	CD_{β}	2.2088e-05	CY_{β}	-0.71622
CL_{P}	4.5559e-07	CD_{P}	5.7184e-06	CY_{P}	0.30911
CL_{Q}	7.1928	CD_{Q}	0.2418	CY_{Q}	-1.1347e-11
CL_{R}	-2.0238e-08	CD_{R}	1.8766e-07	CY_{R}	-0.21411

Roll derivatives :		Pitch derivatives :		Yaw derivatives :	
Cl_{α}	-1.5364e-13	Cm_{α}	0.052209	Cn_{α}	-1.5661e-14
Cl_{β}	0.11536	Cm_{β}	8.5081e-06	Cn_{β}	-0.068092
Cl_{P}	-0.83441	Cm_{P}	2.4044e-06	Cn_{P}	-0.0069725
Cl_{Q}	-2.7804e-11	Cm_{Q}	-2.3204	Cn_{Q}	-1.4538e-12
Cl_{R}	0.0081786	Cm_{R}	1.0266e-07	Cn_{R}	-0.023249

Figure 6.8: Derivatives calculated with use of Tornado VLM

7 STRUCTURAL ANALYSIS

7.1 Calculation method

Due to the use of the biplane design, simplified approach was used to determine structural strength and rigidity. Simplification was based on assumption, that the whole top wing will act as a top flange and the bottom wing as a bottom flange of a spar. Struts bear the forces between the wings in z direction. Sheer stress is transmitted solely by the wires attached to the wing connection points and to the roots of wing struts. Torsional moment from elevon deflection was calculated as it is acting in the place of the endplate and each of top and bottom wings carries its half. Connection points of wings are constructed as a pin supports and does not carry any moment.

7.2 Flight envelope

To calculate required strength of the aircraft it was necessary to determine operational envelope of the aircraft. Based on the requirements, maximal loading factor limits were specified and velocity vs load factor (V-n) diagram was created. For maneuvering envelope maximal load factors were specified as shown in table 7.1. Maximal dive speed V_D was set at 33.3 m/s to incorporate case of flight without the net installed. Considered speeds for V-n diagram are shown in table 7.2. Calculated maneuver speed V_A is in the case of this aircraft higher, than the expected V_C. Gust velocities Ug_{VC} and Ug_{VD} were slightly lowered, in deviation of CS23 rules, due to low operational altitude of the aircraft.

Load factor	-
n_{max}	8.0
n_{min}	3.8

Table 7.1: Maximal loading factors

Speed	m/s
V_D	33.3
V_C	12.0
V_S	7.3
V_A	20.8

Table 7.2: Speeds for V-n diagram

Based on these parameters, maneuver (figure 7.1) and gust (figure 7.2) V-n diagrams were constructed. Because of low gust velocity, it was found, that the Gust envelope does not have effect on the total V-n envelope of the aircraft.

Gust speed	m/s
Ug_{VC}	10
Ug_{VD}	6

Table 7.3: Selected maximal gust velocities Ug

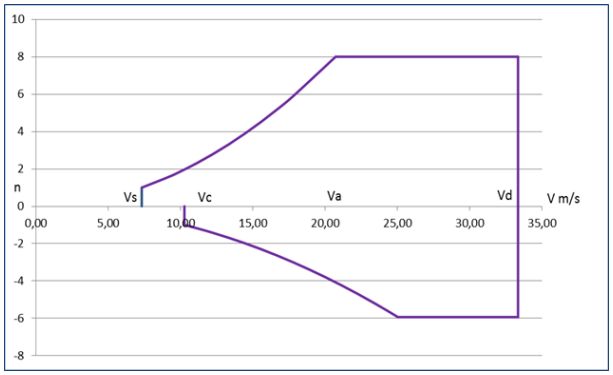

Figure 7.1: Maneuver V-n diagram

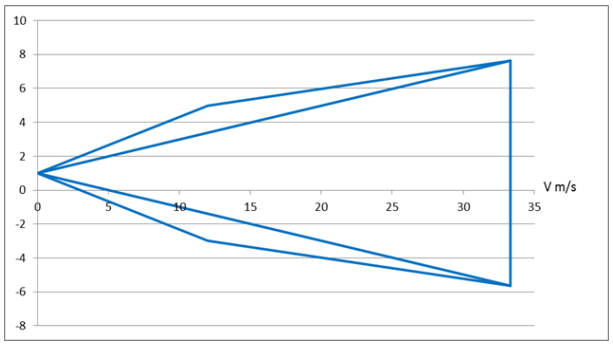

Figure 7.2: Gust V-n diagram

7.3 Wing loading

Using Tornado VLM, aerodynamic loading was calculated for various velocities including V_D. Results were processed by MATLAB code to obtain aerodynamic loading at investigated points of V-n diagram. Largest loading were expected to occur at n_max and V_D. Dependency of C_L on delta (figure 7.4) was used to determine aerodynamic forces with elevons symmetricaly in maximal and minimal deflections.

Most of the values were obtained using Tornado VLM with following adjustments, except Torsional moment, which is not part of output of Tornado. Torsional moment was calculated from shear force, using following equations. Line torsional moment q_{Mk} can be expressed using equation 7.1.

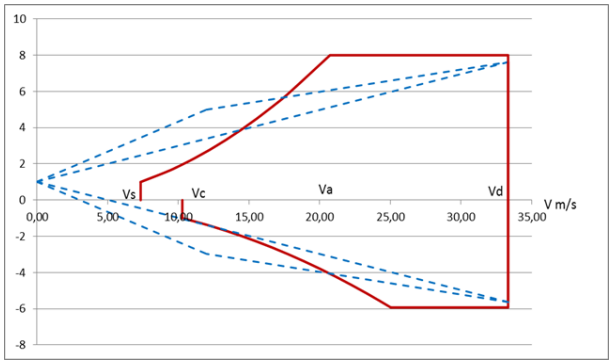

Figure 7.3: Total V-n diagram (Red conture)

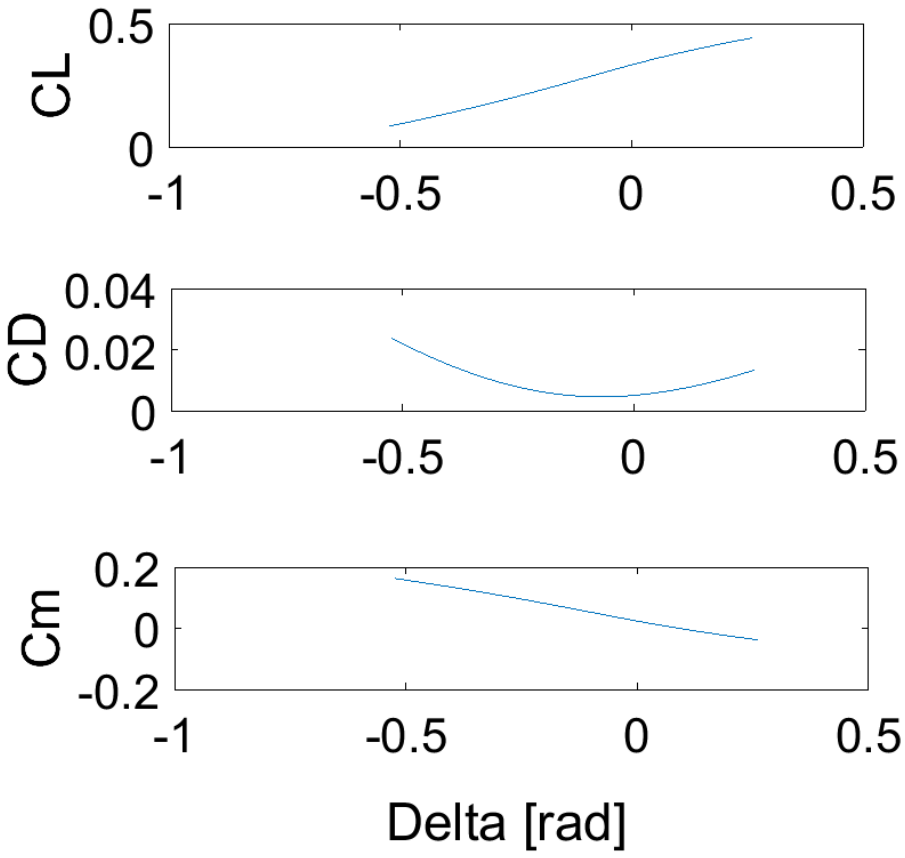

Figure 7.4: Coefficients dependency on deflection angle of elevons

$$q_{Mk}(y) = \frac{1}{2} \cdot \rho \cdot \nu^2 \cdot c_m \cdot c_{(y)^2} \tag{7.1}$$

Root torsional moment for tailed aircraft created by c_m can be calculated by equation 7.2 In case of tailless aircraft and the used airfoil MH-44, c_m is very close to 0, therefore it was assumed that M_{kCm} was also 0. Because of this assumption, shear force was created solely by shear force.

$$M_{kCm}(y) = \int_{\frac{b}{2}}^{y} q_{Mk(y)} \cdot dy \tag{7.2}$$

Torsional moment around 25% axis of root airfoil created by force acting at a lever because of a wing sweep could be calculated using equation 7.3.

$$M_{kT25\%Ck}(y) = \int_{\frac{b}{2}}^{y} T(y) \cdot r(y) \cdot dy \tag{7.3}$$

Which is useful in the case of tailed aircraft, for tailless aircraft, the maximal torsion moment will not occur at the root, but somewhere on the wing. This point was calculated using MATLAB and for this case of loading was found to be at y = 0.4675 m, as can bee seen in figure 7.5

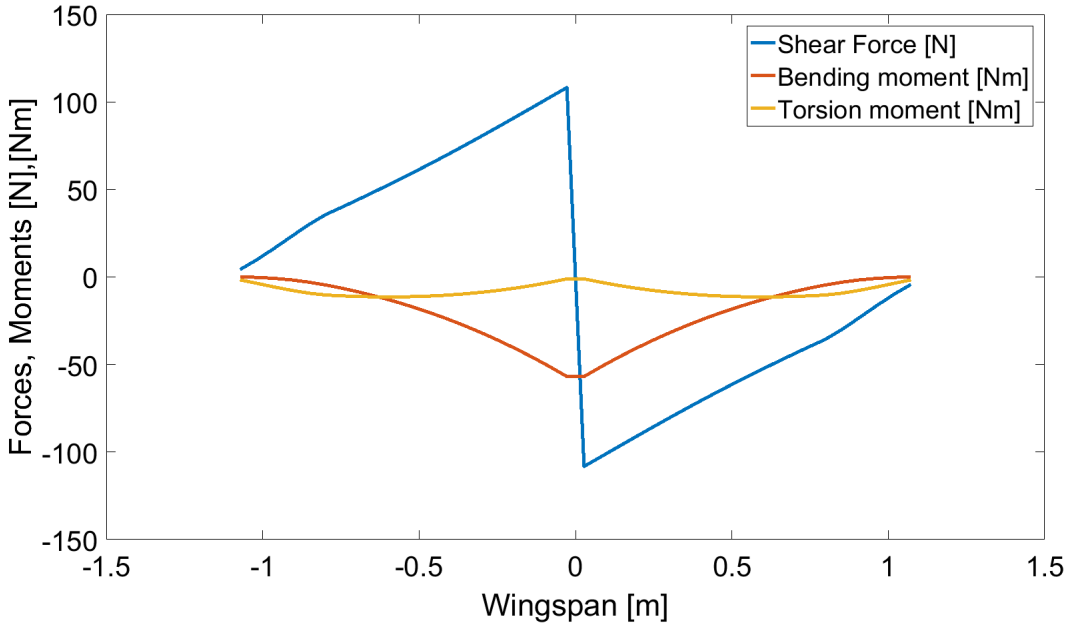

Figure 7.5: Forces and moments at V_D and n_{max} with fully deflected elevons at 15°

Shear flow from torsion could be calculated using Bredt's formula 7.4 which applies for thin-walled structures.

$$q_k = \frac{M_k}{2 \cdot U} \tag{7.4}$$

As the wing is designed mainly for easy manufacturing to prove aerodynamic characteristics of the aircraft, and because of low loading in case of tailless aircraft, there is no surprise the factor of safety for torsion was found to be 903.

The wing strength was calculated using equations and , but the loading was again found to be insignificant, because of connection point design as is explained further.

$$N = \frac{M_x}{h_e} = F \cdot \sigma \tag{7.5}$$

$$F_h \geq \frac{M_x}{\sigma_d \cdot h_e} \tag{7.6}$$

As the wing connection points are designed as a simple pin connections, there is no transfer of bending moment to the fuselage. For the computation, the whole wing structure was solved as a truss structure with the diagonal wires carrying the most of the stress. The angle of the wire is 54,7°. The wire used is a nylon braided fishing line, which is good for such use, because of its very low relative strain. Because of the simplification, safety factor used was 2.6 which led to the wire being 1 mm in diameter.

8 VISUALIZATION

After finishing the structural calculations, models of the aircraft were created in system CATIA. Whole aircraft can be seen on figure 8.1. The trap with the opening mechanism is visible on rear view of the aircraft on figure 8.2. Detail of wing connection point of bottom wing with wire connection point above is shown on figure 8.3. Wires supporting the wings can be seen on figure 8.6.

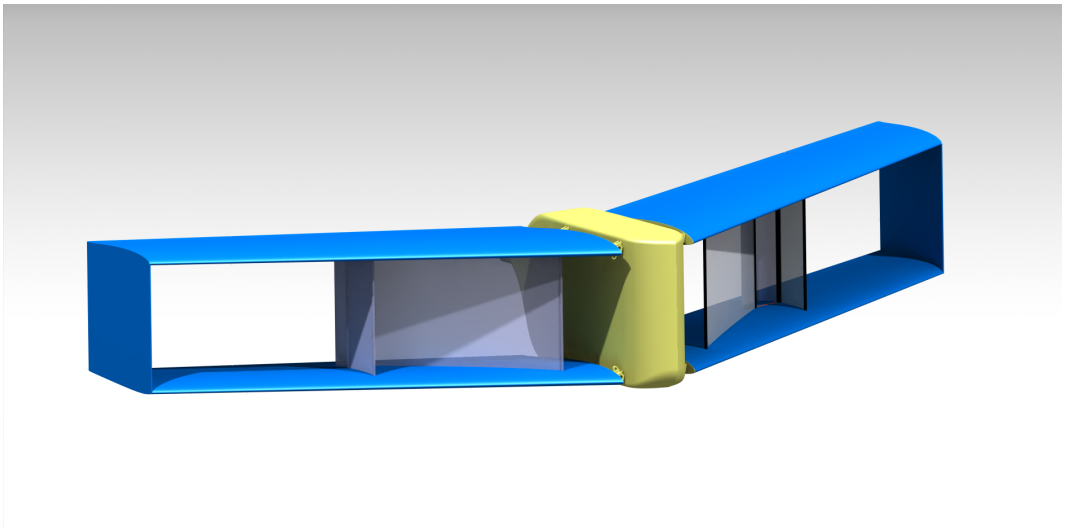

Figure 8.1: Insect collecting unmanned aerial vehicle from front

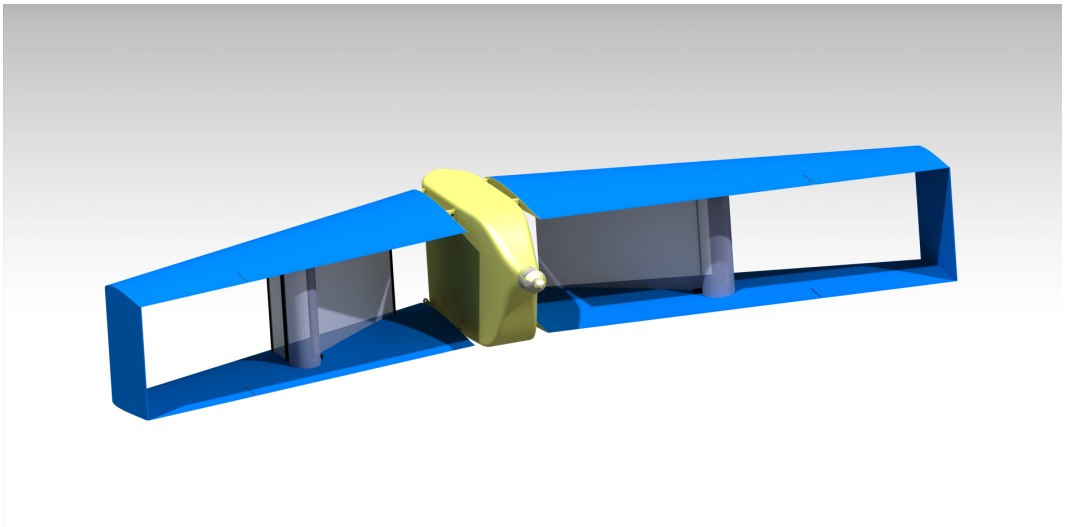

Figure 8.2: Rear view of the aircraft

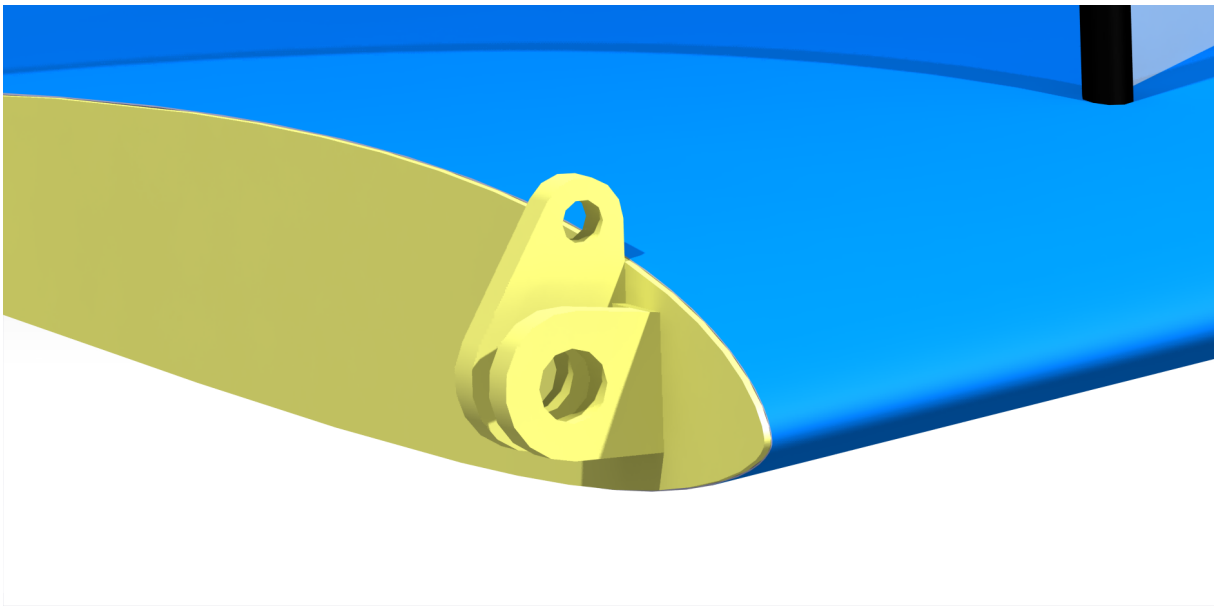

Figure 8.3: Wing connection point

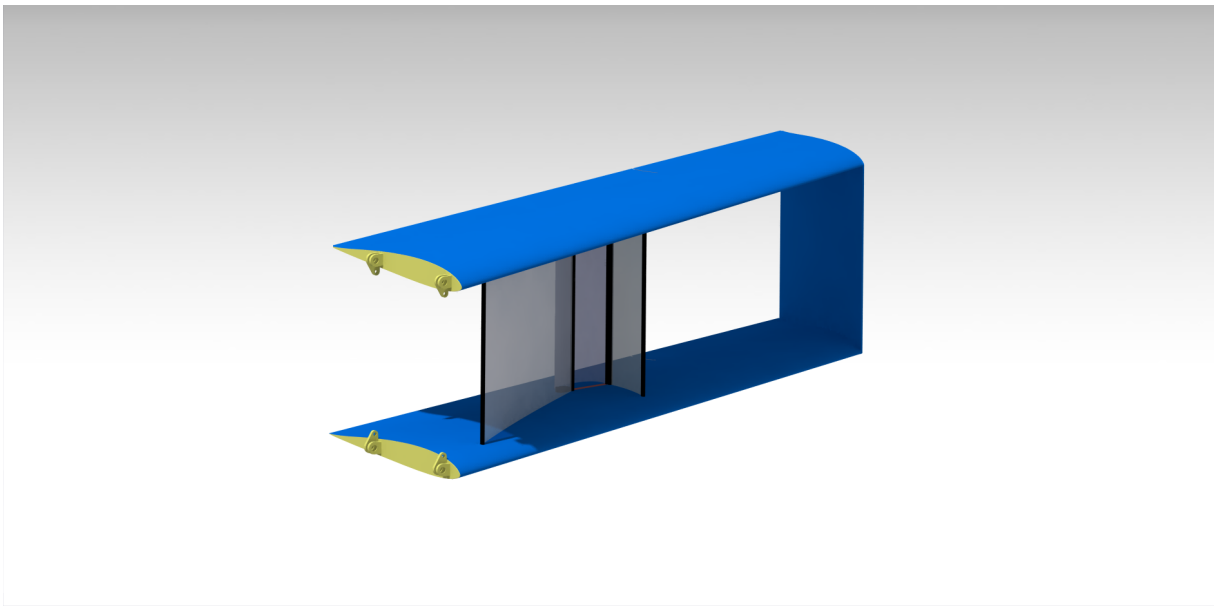

Figure 8.4: Wing detail viewed from front

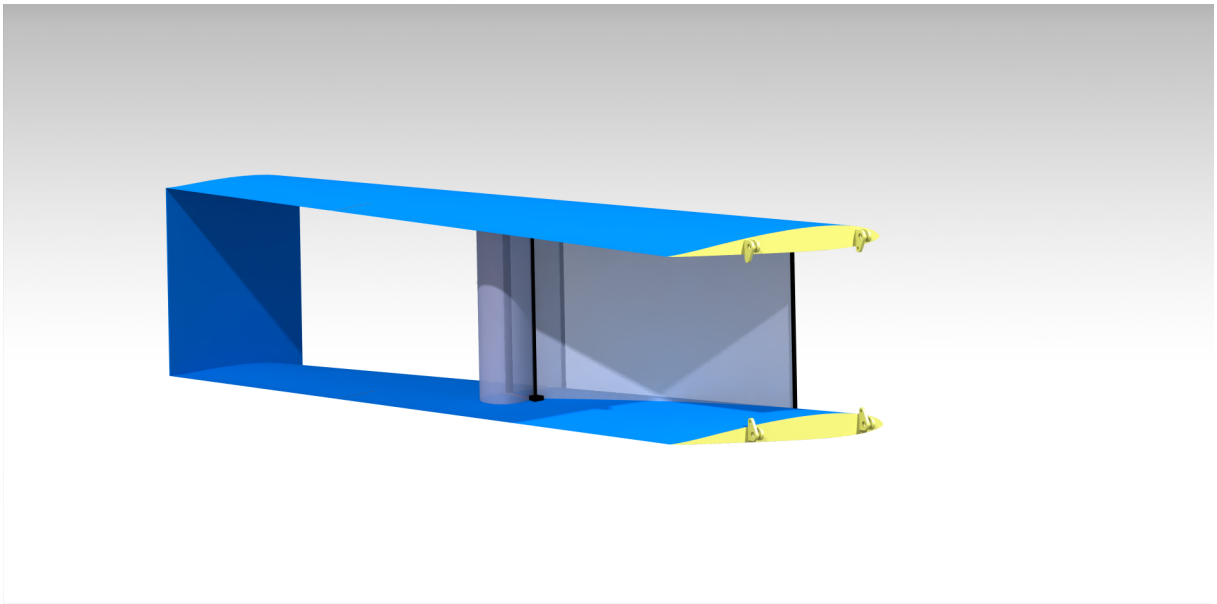

Figure 8.5: Wing detail from back

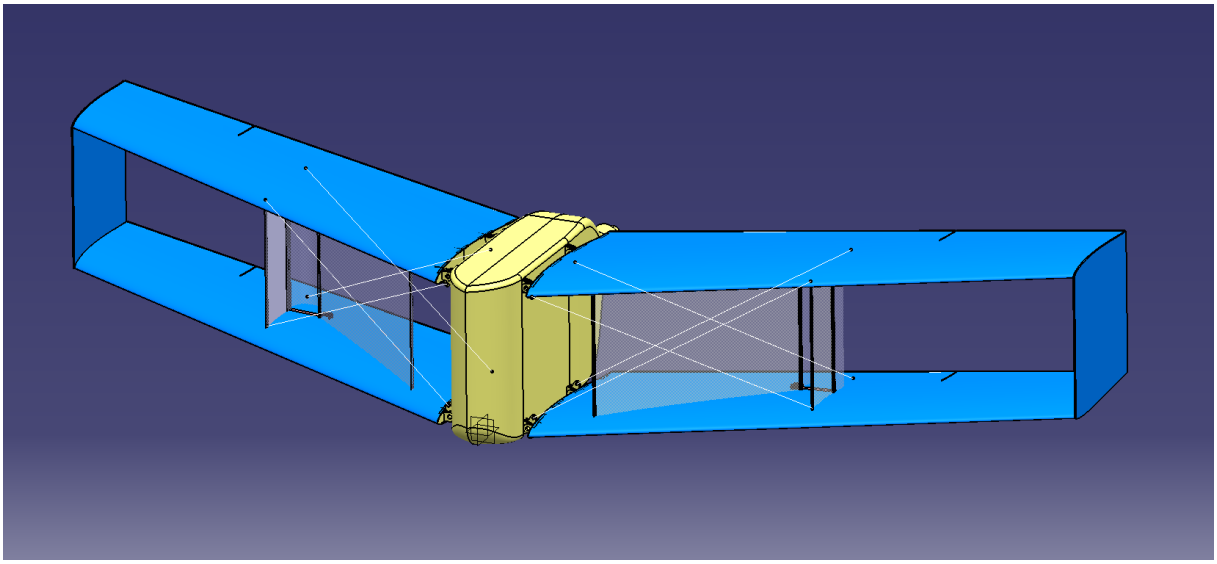

Figure 8.6: Aircraft with visible wires

9 OVERALL SUMMARY AND FUTURE WORK RECOMMENDATIONS

There are several important steps for future work on Blue Whale UAV, which will follow this work. After tweaking the design, which will have to happen, the aircraft will be manufactured. Flight tests are expected to occur without the full battery load and without the trap installed. After verification (or refutation) of stability characteristics of aircraft, flights are to be conducted with the net and find difference in behavior with and without the net.

Quite useful for would be placing pressure measurement device at various places behind the net to verify calculated pressure differences.

Problem of the aircraft is its very low cruise speed with heavy loading, this issue might be overcome by using combustion engine, which can have higher power to weight ratio [16]. Another way of solving the heavy loading can be consideration of using canard configuration, which would enable use of airfoils with higher lift coefficient on the main wing.

Parameter	Value	Unit
Airfoil	MH 44	
Wingspan	2.2	m
Wing Area (one wing)	0.715	m^2
Wing Area	1.430	m^2
Root chord	0.4	m
Tip chord	0.25	m
Aspect Ratio		-
Tapering	0.659	-
Leading edge sweep	24	$^\circ$
Wing twist	-3	$^\circ$
MAC length	0.33	m
Center of gravity x position	0.27	m
Aircraft gross weight	5.275	kg
Battery weight	2.5	kg
Trap frontal area	0.25	m^2
V_D	33.3	m/s
V_C	12.0	m/s
V_S	7.3	m/s
V_A	20.8	m/s
n_{max}	8.0	m/s
n_{min}	3.8	m/s

Table 9.1: Summary of aircraft parameters

10 CONCLUSION

Unmanned aerial vehicle of wingspan of 2.2 m able to collect aeroplankton was designed. Aircraft uses tailless biplane concept with insect traps placed between the wings. Traps can be opened and closed during the flight. Maximal flight time is 40 minutes at cruise speed. Aircraft gross weight is 5.275 kg of which 2.5 kg is reserved for battery, as it was found that for the aircraft to provide selected tasks, enormous power amount is needed. Airplane can be disassembled to three separate parts for transportation. Computations were done by use of MATLAB script written by the author (attached) and Tornado VLM script. 3D models of aircraft were created using Catia.

REFERENCES

[1] A-10 inboard profile. In: *Wikipedia* [online]. [ref. 2017-05-24]. Available from: https://upload.wikimedia.org/wikipedia/commons/thumb/d/da/A-10_Cross_Section.jpg/1280px-A-10_Cross_Section.jpg

[2] *Airfoil Tools: Search 1636 airfoils* [online]. 2017 [ref. 2017-05-24]. Available from: http://airfoiltools.com

[3] BAILEY, B.J, J.I MONTERO, J.Pérez PARRA, A.P ROBERTSON, E. BAEZA a R. KAMARUDDIN. Airflow Resistance of Greenhouse Ventilators with and without Insect Screens. *Biosystems Engineering.* 2003, Vol. 86, no. 2, p. 217-229. DOI: 10.1016/S1537-5110(03)00115-6. ISSN 15375110. Available from: http://linkinghub.elsevier.com/retrieve/pii/S1537511003001156

[4] BRUNDRETT, E. Prediction of Pressure Drop for Incompressible Flow Through Screens. *Journal of Fluids Engineering.* 1993, Vol. 115, no. 2, p. 239-242. DOI: 10.1115/1.2910130. ISSN 00982202. Available from: http://FluidsEngineering.asmedigitalcollection.asme.org/article.aspx?articleid=1427522

[5] COLEMAN, W.S. The Characteristics of Roughness from Insects as Observed for Two-Dimensional, Incompressible Flow Past Airfoils. *Journal of the Aerospace Sciences.* 1959, Vol. 26, no. 5, p. 264-280. DOI: 10.2514/8.8044. ISSN 1936-9999. Available from: http://arc.aiaa.org/doi/10.2514/8.8044

[6] COLEMAN, W.S. Roughness due to insects. In:*Boundary Layer and Flow Control.* Elsevier, 1961, s. 682. DOI: 10.1016/B978-1-4832-1323-1.50006-3. ISBN 9781483213231. Available from: http://linkinghub.elsevier.com/retrieve/pii/B9781483213231500063

[7] ČESKÁ REPUBLIKA. Doplněk X - Bezpilotní systémy. In: *Letecký předpis - Pravidla létání.* 2014. Available from: http://lis.rlp.cz/predpisy/predpisy/dokumenty/L/L-2/data/effective/doplX.pdf

[8] DANĚK, Vladimír. *Mechanika letu.* Brno: Akademické nakladatelství CERM, 2009. ISBN 978-80-7204-659-1.

[9] FALKOVICH, G. *Fluid mechanics: a short course for physicists.* New York: Cambridge University Press, 2011. ISBN 11-070-0575-2.

[10] *Flying wing CG calculator* [online]. [ref. 2017-05-24]. Available from: http://fwcg.3dzone.dk

[11] FREEMAN, J.A. Studies in the Distribution of Insects by Aerial Currents. *The Journal of Animal Ecology.* 1945, Vol. 14, no. 2, p. 128-154. DOI: 10.2307/1389. ISSN 00218790. Available from: http://www.jstor.org/stable/1389

[12] GLICK, P.A. The Distribution of Insects, Spiders, and Mites in the Air. *Technical Bulletin.* 1939, no. 637, 151 p.

[13] GLICK, P.A. Review of Collections of Lepidoptera by Airplane. *Journal of the Lepidopterists' Society.* 1965, Vol. 19, no. 3, p. 130-137. ISSN 0024-0966.

[14] HARDY, A. C. a P. S. MILNE. Studies in the Distribution of Insects by Aerial Currents. *The Journal of Animal Ecology.* 1938, Vol. 7, no. 2, p. 199-229. DOI: 10.2307/1156. ISSN 00218790. Available from: http://www.jstor.org/stable/1156

[15] HEPPERLE, Martin. *Aerodynamics of Model Aircraft* [online]. 16.02.08 [ref. 2017-05-24]. Available from: http://www.mh-aerotools.de/airfoils/index.htm

[16] HEPPERLE, Martin. *Electric flight-potential and limitations.* 2012. Available from: http://elib.dlr.de/78726/1/MP-AVT-209-09.pdf

[17] CHAPMAN, J.W., D.R. REYNOLDS, A.D. SMITH, E.T. SMITH a I.P. WOIWOD. An aerial netting study of insects migrating at high altitude over England. *Bulletin of Entomological Research.* 2004, Vol. 94, no. 02, p. 123-136. DOI: 10.1079/BER2004287. ISSN 0007-4853. Available from: http://www.journals.cambridge.org/abstract_S0007485304000148

[18] CHAPMAN, J.W., V. Alistair DRAKE a D.R. REYNOLDS. Recent Insights from Radar Studies of Insect Flight. *Annual Review of Entomology.* 2011, Vol. 56, no.1, p. 337-356. DOI: 10.1146/annurev-ento-120709-144820. ISSN 0066-4170. Available from: http://www.annualreviews.org/doi/10.1146/annurev-ento-120709-144820

[19] JENKINS, Dennis R. *Fairchild-Republic A/OA-10 Warthog.* North Branch, MN: Specialty Press, 1998. ISBN 9781580071970.

[20] KANG, Hantae, Nicola GENCO a Aaron ALTMAN. Gap and Stagger Effects on Biplanes with End Plates: Part I. *47th AIAA Aerospace Sciences Meeting including The New Horizons Forum and Aerospace Exposition.* Reston, Virigina: American Institute of Aeronautics and Astronautics, 2009. DOI: 10.2514/6.2009-1085. ISBN 978-1-60086-973-0. Available from: http://arc.aiaa.org/doi/10.2514/6.2009-1085

[21] KOK, M., E.F. TOBIN, P. ZIKMUND, D. RAPS a T.M. YOUNG. Laboratory testing of insect contamination with application to laminar flow technologies, Part I: Variables affecting insect impact dynamics. *Aerospace Science and Technology.* 2014, Vol. 39, p. 605-613. DOI: 10.1016/j.ast.2014.07.002. ISSN 12709638. Available from: http://linkinghub.elsevier.com/retrieve/pii/S127096381400131X

[22] LAWS, E.M. a J.L. LIVESEY. Flow Through Screens. *Annual Review of Fluid Mechanics.* 1978, Vol. 10, no. 1, p. 247-266. DOI: 10.1146/annurev.fl.10.010178.001335. ISSN 0066-4189. Available from: http://www.annualreviews.org/doi/10.1146/annurev.fl.10.010178.001335

[23] MATHESON, Tom. Motor Planning: Insects Do It on the Hop. *Current Biology.* 2008, Vol. 18, no. 17, R742-R743. DOI: 10.1016/j.cub.2008.07.039. ISSN 09609822. Available from: http://linkinghub.elsevier.com/retrieve/pii/S0960982208009457

[24] NICKEL, Karl a Michael WOHLFAHRT. *Tailless aircraft in theory and practice.* London: Edward Arnold, 1994. ISBN 03-406-1402-1.

[25] PAULSON, Gregory S. *Handbook to the construction and use of insect collection and rearing devices: a guide for teachers with suggested classroom applications.* Dordrecht, The Netherlands ; New York: Springer, 2005. ISBN 978-140-2029-745.

[26] PENNISI, Elizabeth. Like birds, insects may travel in sync with the seasons. *Science.* 2016, Vol. 354, no. 6319, p. 1515. DOI: 10.1126/science.354.6319.1515. ISSN 0036-8075. Available from: http://www.sciencemag.org/lookup/doi/10.1126/science.354.6319.1515

[27] Pixhawk. In: *Unmanned Tech* [online]. [cit. 2017-05-26]. Available from: https://cdn6.bigcommerce.com/s-xkoep7/product_images/uploaded_images/pic-prod-pixhawk1.jpg?t=1429711272

[28] RADECKI, Alan. BD-1B. In: Vintage air [online]. 2015 [cit. 2017-05-28]. Available from: http://vintageairphotos.blogspot.cz/2015/04/the-birth-of-american-flying-wing.html

[29] *Precision Woven Synthetic* Monofilament Fabrics. Switzerland: Sefar, 2015.

[30] SIEGMANN, Hartmut. *Aerodesign* [online]. 2016 [ref. 2017-05-24]. Available from: https://www.aerodesign.de

[31] SMITS, Alexander J. a Jean-Paul. DUSSAUGE. *Turbulent shear layers in supersonic flow.* 2nd ed. New York: Springer, c2006. ISBN 03-872-6140-0.

[32] TEITEL, M., D. DVORKIN, Y. HAIM, J. TANNY a I. SEGINER. : Effects of screen inclination and porosity. *Biosystems Engineering.* 2009, Vol. 104, no. 3, p. 404-416. DOI: 10.1016/j.biosystemseng.2009.07.006. ISSN 15375110. Available from: http://linkinghub.elsevier.com/retrieve/pii/S1537511009002256

[33] *Tornado: a Vortex Lattice method implemented in MATLAB* [online]. [ref. 2017-05-24]. Available from: http://tornado.redhammer.se

[34] WORTHEN, Wade B. Latitudinal Variation in Developmental Time and Mass in Drosophila melanogaster. *Evolution.* 1996, Vol. 50, no. 6, p. 2527. DOI: 10.2307/2410721. ISSN 00143820. Available from: http://www.jstor.org/stable/2410721?origin=crossref

11 LIST OF USED SYMBOLS

C_D	Drag coefficient
V_A	Maneuver speed
V_C	Cruise speed
V_D	Dive speed
V_S	Stall speed
Ug_{VC}	Gust velocity at VC
Ug_{VD}	Gust velocity at VD
n_{max}	Maximal loading factor
n_{min}	Minimal loading factor
μm	Dynamic viscosity
ϕ	Angle of screen
λ	Gass constant
v	Free stream velocity
ν	Kinematic viscosity
v	Mesh thread diameter
C	Sutherland's constant
T	Temperature
a	Mesh porosity
ρ	Mass density
r	Lever of Shear force
c_m	Moment coefficient
c	Chord lenght
M_{kT}	Torsional moment from shear force
M_{kCm}	Toarsional moment from washout
$M_{kT25\%Ck}$	Torsional moment around 25% axis
b	Wingspan

q_k	Shear flow
M_k	Torsional moment
U	Area inside thin walled structure
F_h	Flange area
M_x	Bending moment
σ_d	Maximal permissible stress
h_e	Effective height of the beam
N	Normal force
F	Force
σ	Stress

LIST OF FIGURES

2.1 Stinson Detroiter SM1 monoplane, specially constructed for insect collecting [12] . . . 9
2.2 A single-compartment insect trap adapted for use on the leading edge of the lower wing of a biplane [12] . . . 10
2.3 Insect trap, steel rails extend from rear of the cabin to the wing strut, where the net is placed in collecting regime. [12] . . . 11
2.4 Closed net being pulled up, attached to the kite [12] . . . 11
2.5 Vertical looking radar and harmonic radar [18] . . . 12
3.1 D.Melanogaster after impact beyond its rupture velocity [21] . . . 14
4.1 A-10 Thunderbolt II [1] . . . 17
4.2 Brugess Dunne BD-1B - designed by John William Dunne [28] . . . 18
4.3 Pixhawk flight control [27] . . . 20
5.1 Net at different angles . . . 23
5.2 Reynolds number of meshes . . . 24
5.3 Pressure loss coefficient of meshes . . . 24
5.4 Pressure difference of meshes . . . 25
5.5 Pressure difference of selected mesh . . . 25
5.6 Drag as a function of net frontal area . . . 26
5.7 Lift induced drag . . . 26
5.8 Parasitic power . . . 27
5.9 Comparison of induced power and parasitic power caused by the net . . . 27
5.10 Battery weight required by the parasitic power of the net . . . 28
5.11 Battery weight required by parasitic power for selected free stream velocities . . . 28
6.1 Airfoil MH 44 [2] . . . 31
6.2 Comparison of selected airfoils at low Re [2] . . . 31
6.3 MH 44 polar at relevant Re . . . 32
6.4 Comparison of Cl and Cm by angle of attack at relevant Re . . . 32
6.5 Location of transition point and dependance of Cl/Cd on angle of attack 33
6.6 Top view of the wing created using [10] . . . 34
6.7 Pressure difference on the wing created using Tornado VLM script . . . 34
6.8 Derivatives calculated with use of Tornado VLM . . . 35
7.1 Maneuver V-n diagram . . . 37
7.2 Gust V-n diagram . . . 37
7.3 Total V-n diagram (Red conture) . . . 38
7.4 Coefficients dependency on deflection angle of elevons . . . 38
7.5 Forces and moments at V_D and n_{max} with fully deflected elevons at 15° 39
8.1 Insect collecting unmanned aerial vehicle from front . . . 41
8.2 Rear view of the aircraft . . . 41
8.3 Wing connection point . . . 42
8.4 Wing detail viewed from front . . . 42
8.5 Wing detail from back . . . 43
8.6 Aircraft with visible wires . . . 43

LIST OF TABLES

3.1 Table of requirements 15
4.1 Estimated mass of individual segments 19
5.1 Table of mesh materials 22
6.1 Narrow selection of considered airfoils [30] 30
6.2 Aircraft geometric parameters 33
7.1 Maximal loading factors 36
7.2 Speeds for V-n diagram 36
7.3 Selected maximal gust velocities Ug 37
9.1 Summary of aircraft parameters 44